UNIVERSIDADE DE LISBOA

FACULDADE DE FARMÁCIA

NANOFORMULATIONS OF A POTENT AQUAPORIN-3 INHIBITOR WITH CYTOTOXIC EFFECT AGAINST CANCER CELL LINES

Mariana Vieira de Almeida Nave

Dissertação de Mestrado

Mestrado em Ciências Biofarmacêuticas

2013

UNIVERSIDADE DE LISBOA

FACULDADE DE FARMÁCIA

NANOFORMULATIONS OF A POTENT AQUAPORIN-3 INHIBITOR WITH CYTOTOXIC EFFECT AGAINST CANCER CELL LINES

Mariana Vieira de Almeida Nave

Dissertação de Mestrado orientada por:

Prof. Doutora Graça Soveral, Faculdade de Farmácia, Universidade de Lisboa

Doutora Maria Manuela Gaspar, Faculdade de Farmácia, Universidade de Lisboa

Doutor Rui E. Castro, Faculdade de Farmácia, Universidade de Lisboa

Mestrado em Ciências Biofarmacêuticas

2013

Communications in scientific meetings

Nave MA, Gaspar MM, Castro RE, Rodrigues CM, Soveral G. (2013) "Nanoformulations of a potent Aquaporin-3 inhibitor with cytotoxic effect against cancer cell lines", poster presented at the 5th iMed.UL Post-Graduate Students Meeting, Faculdade de Fármacia Universidade de Lisboa, p. 43, Lisboa, Portugal.

A ti minha pequenina… mãe com açúcar.

Das pessoas que mais me amou e sem dúvida a que mais vibrou com cada conquista minha, por mais pequena que fosse. Sei que estás comigo.
Por tudo… esta "vitória" também é tua.

"Quod per sortem sternit fortem"

Agradecimentos

À Professora Teresa Moura. Foi a primeira pessoa que, ainda antes de terminar a licenciatura, depositou confiança em mim. Foi o meu primeiro passinho ao encontro da realização profissional e claro, pessoal. Foi também a pessoa que me apresentou as AQPs e...a Professora Graça. Muito grata por tudo Teresa.

Logo de seguida quero agradecer à Professora Graça pela oportunidade de me receber no grupo e claro, avançar com este projecto que desde logo abracei com entusiasmo. Agradeço por tudo o que me ensinou, por toda a disponibilidade, confiança, opinião e orientação.

À Professora Cecília Rodrigues agradeço pela oportunidade de colaboração, tendo-me permitido realizar parte do trabalho no seu grupo.

Ao Professor Rui, pela orientação e apoio ao longo desta minha etapa. Para além da partilha de conhecimento, um obrigado pela boa disposição e pensamento positivo constantes.

À Doutora Manuela Gaspar… "Chefinha", o meu eterno obrigado por toda a disponibilidade, partilha, orientação e dedicação! Agradeço também a compreensão demonstrada num momento menos feliz da minha vida.

Quero deixar um agradecimento também às várias pessoas com quem partilhei oxigénio, algumas sábias palavras (muitas!) e saudáveis gargalhadas nestes últimos meses. Mesmo a brincar há sempre alguma coisa a aprender e quando estamos dispostos a aprender todas as pessoas com quem nos cruzamos têm algo a ensinar.

Cláudia agradeço-te o conhecimento que partilhaste e a paciência que demonstraste quando comecei o trabalho no laboratório. À Paulinha e Ana Madeira agradeço principalmente pela paciência para os meus constantes e típicos "porquês". Ambas me ensinaram muito! Necas... não me esqueço de ti! Tens aqui uma amiga-jukebox!

Susana, o que teria sido de mim nos primeiros tempos que passei no laboratório se não fosse a tua constante disponibilidade?! Obrigado pela partilha, boa disposição e pelos momentos de descontracção e pura parvoíce! Maria, Joana, Rui, Xana, Ana… Obrigado a cada um de vocês. Proporcionaram bons momentos!

Aos meus amigos de mestrado, principalmente Anocas, Ceci e Vasco, quero deixar um agradecimento muito especial. Ter-vos conhecido foi um dos grandes pontos de viragem neste meu caminho. A vossa amizade importa muito!

Hugo...faço questão de deixar um beijinho enorme. Foste um dos pilares da minha sanidade mental durante este último ano. Um obrigado bem lamechas para ti pela tua dedicação e

amizade sincera. Das várias pessoas com quem me cruzei até hoje, és sem dúvida uma das que maior coração tem (e paciência!).

Bruno, a ti agradeço todo o amor e carinho… toda a amizade e dedicação mas acima de tudo por toda a paz com a qual constantemente me envolves. Obrigado do fundo do coração!

Quero agradecer também a duas pessoas que foram essenciais para ser o que hoje sou: ao meu "amigo do coração" André… não preciso de te dizer muito. Ensinaste-me a ver a vida de uma maneira muito mais cheia e iluminada. Hoje sinto-me mais preenchida e ao mesmo tempo mais leve. Sim, a nossa amizade perdurará. A ti Miguel, agradeço a paciência, dedicação e amizade que dispensaste ao longo de vários anos. Tiveste um papel central na minha formação tanto a nível pessoal como profissional. É impossível esquecer o que por mim fizeste. A vocês os dois o meu eterno e sentido obrigado.

A todos os meus restantes amigos, não menos importantes para o meu crescimento e evolução constantes... Obrigado pelo respeito, carinho, amor, sinceridade e compreensão.

Aos meus tios e primos que sempre me apoiaram. Destaco o meu tio Lipi que, apesar de não me ver terminar esta etapa, me ensinou que a "sorte vale sempre muito pouco".

Agradeço também do fundo do coração à minha tia Maria Helena sem a qual esta tinta nestas folhas, não faria qualquer sentido. Eternamente grata minha tia!

Aos meus pais… obrigado por toda a confiança que em mim depositam desde pequena. Obrigado pelo apoio, amor, carinho e amizade incondicionais! Obrigado por todos os "Não!", raspanetes e castigos. Neste mesmo parágrafo incluo-te a ti meu irmão. És o meu maior e mais bonito reflexo… a melhor parte de mim. Porque são e serão sempre o meu porto de abrigo, a minha família mas acima de tudo os meus melhores amigos. Amo-vos!

Table of Contents

List of Figures

List of Tables

Resumo

As aquaporinas (AQPs) são proteínas transmembranares responsáveis pelo transporte de água e de outros solutos, como o glicerol, através das membranas plasmáticas.

Estes transportadores entraram recentemente na lista de possíveis alvos terapêuticos na área da oncobiologia uma vez que a sua sobre-expressão está associada a diferentes tipos de cancro. Em particular a aquaporina-3 (AQP3), uma aquagliceroporina abundantemente expressa ao nível da epiderme, é agora tida como "chave" na tumorigénese e quimioresistência em casos de cancro de pele. Deste modo, as AQPs estão a ganhar relevância enquanto alvos biológicos na terapia do cancro e os seus modeladores a reunir interesse por parte da indústria farmacêutica.

Recentemente, o nosso grupo descreveu diferentes compostos baseados em iões metálicos como inibidores potentes e selectivos da AQP3 humana. Em particular, o composto derivado de cobre(II) da fenantrolina – Cuphen – demonstrou ter efeito inibitório selectivo sobre a permeabilidade ao glicerol quando testado em eritrócitos humanos, mostrando-se assim promissor para administração *in vivo.*

Por conseguinte, este trabalho teve como principal objectivo o desenvolvimento de um sistema de veiculação adequado, baseado em estruturas lipídicas artificiais, nomeadamente lipossomas, de modo a poder permitir uma estabilização de inibidores da AQP3, alterando o seu perfil de biodistribuição *in vivo,* proporcionando um direccionamento preferencial para as áreas de interesse terapêutico aquando da sua administração.

Assim, e recorrendo à linha celular tumoral A431, derivada de carcinoma epidermoide humano, e que apresenta sobre-expressão endógena de AQP3, foi avaliado o potencial citotóxico de diferentes compostos metálicos inibidores da AQP3. Após identificação do composto mais citotóxico, o Cuphen (([Cu(phen)Cl_2]Cl (phen = 1,10-fenantrolina)), já descrito como inibidor selectivo da AQP3 em eritrócitos humanos, foi seleccionado para incorporação em lipossomas de escala nanométrica (inferior a 0.2 µm). Usando diferentes composições lipídicas foram obtidas eficiências de incorporação de cerca de 50%.

O efeito citotóxico do Cuphen, nas formas livre e lipossomal, foi avaliado na linha celular A431 e numa linha de cancro de cólon de murganho (C26). Para a forma livre, obtiveram-se valores de IC_{50} de 3.0 ± 0.4 µM e 1.8 ± 0.1 µM para as linhas A431 e C26, respectivamente, após 72h de incubação. A incorporação do Cuphen em lipossomas permitiu a preservação do seu efeito citotóxico ($IC_{50} \leq 10$ µM após 72h de incubação).

É ainda de referir que os lipossomas vazios não apresentaram qualquer efeito a nível da viabilidade das células testadas.

Com base nestes resultados, o estudo de formulações lipossomais para encapsular este inibidor deve ser aprofundado e o estabelecimento de um modelo animal de melanoma humano deve ser considerado, por forma a avaliar o efeito terapêutico deste composto metálico.

Palavras-chave: Aquaporina-3, cancro, Cuphen, lipossomas.

Abstract

Aquaporins (AQPs) are a family of small transmembrane proteins that facilitate the transport of water and other solutes, such as glycerol, across the cell plasma membrane. AQPs are now part of the expanding list of effectors in cancer biology after establishment of positive correlations between the histological tumor grade and their aberrant expression in different tumor types. In particular, the AQP3 aquaglyceroporin, which is abundantly expressed in skin keratinocytes, is now seen as a key player in skin tumorigenesis and chemoresistance. Therefore, AQPs are gaining relevance as drug targets for cancer therapy and AQPs' modulators are gathering interest from the pharmaceutical industry.

Our group recently reported different metallodrugs as potent and selective human AQP3 inhibitors for further exploitation on *in vivo* studies. Pursuing this idea, this work had as major aim the development of appropriate drug carrier systems based on artificial closed structures formed by lipid bilayers – liposomes – that may stabilize AQP3 inhibitors and improve *in vivo* delivery.

With this aim, a cytotoxic screening using different AQP3 inhibitors against a human epidermoid carcinoma cell line (A431), presenting endogenous overexpression of AQP3, was performed. Cuphen ($[Cu(phen)Cl_2]Cl$ (phen = 1,10-phenantroline)), previously shown to selectively inhibit AQP3 glycerol transport in human red blood cells, was selected as the most promising inhibitor and incorporated in liposomes in a nanometric scale (below 0.2 μm). Using different lipid compositions, incorporation efficiencies of approximately 50% were achieved. The *in vitro* cytotoxic effect of Cuphen, in both free and liposomal forms, was assessed in the A431 and the C26 murine colon cancer cell lines. In the free form, the IC_{50} obtained was 3.0 ± 0.4 μM and 1.8 ± 0.1 μM for the A431 and for C26, respectively, after 72h of incubation. The incorporation of Cuphen in liposomes was able to preserve the cytotoxic effect of this AQP3 inhibitor ($IC_{50} \leq 10$ μM after 72h of incubation). Moreover, unloaded liposomes did not exert any effect on the viability of these cancer cells.

In view of these *in vitro* results, more liposomal formulations should be tested and the establishment of a murine melanoma model to evaluate the therapeutic effect of Cuphen formulations should be considered.

Keywords: Aquaglyceroporin-3, cancer, Cuphen, liposomes.

Abbreviations and Symbols

(Cuphen/Lip)i	Initial Cuphen to lipid ratio
(Cuphen/Lip)f	Final Cuphen to lipid ratio
$t_{1/2}$	Half-life time
AQP	Aquaporin
Au	Gold
AU	Arbitrary Units
bipy	2,2'-bipyridine; bipyridyl
Chol	Cholesterol
Cisplatin	*cis*-diammine-dichloro platinum(II)
Cu	Copper
dien	Diethylendiamine
DMEM	Dulbecco's modified Eagle's medium
DMPC	Dimyristoyl phosphatidylcholine
DMSO	Dimethyl sulfoxide
DPPC	Dipalmitoyl phosphatidylcholine
DRV	Dehydration-rehydration vesicles
I.E.	Incorporation Efficiency
EtOH	Absolute ethanol
GI	Gastrointestinal
HEPES	4-(2-hydroxyethyl)-1-piperazineethanesulfonic acid
IC_{50}	Half-inhibitory concentration
LCL	Long-circulating liposomes
Lip	Lipid
MPS	Mononuclear phagocytic system
MTS	3-(4,5-dimethylthiazol-2-yl)-5-(3-carboxymethoxyphenyl)-2-(4-sulfophenyl)-2H-tetrazolium, inner salt

MW	Molecular weight
NaCl	Sodium chloride
n.d.	Not determined
NK	Not known
n.s.	Not significant
nm	Nanometer
RPMI	Roswell Park Memorial Institute
PBS	Phosphate buffered saline
PC	Phosphatidylcholine
PEG	Polyethylene glycol
Phen	1,10-phenantroline; phenantroline
P.I.	Polydispersity index
$\mathbf{PO_4^{-3}}$	Phosphate
$\mathbf{R^2}$	Linear correlation coefficient
RBCs	Red blood cells
SA	Octadecylamine; n-Stearylamine
S.D.	Standard deviation
S.E.	Standard error
Tc	Phase transition temperature
terpy	2,2':6',2"- terpyridine; terpyridine
Zeta Pot.	Zeta Potential

1. Introduction

1.1. Aquaporins

Aquaporins (AQPs) are a family of small (≈30 kDa) ubiquitous transmembrane proteins that facilitate the bidirectional transport of water and small uncharged molecules such as glycerol or urea and, in particular cases, ammonia, carbon dioxide and hydrogen peroxide, across the lipid bilayer. (Agre, 1993; Wu, 2007)

The first water channel (AQP1) was reported in 1992 by Preston and co-workers, after purification and subsequent characterization of a protein isolated from red blood cells (RBCs) in *Xenopus* oocytes (Preston, 1992) and its reconstitution into liposomes. (Zeidel, 1992) Since then, several AQPs were identified from yeast, plants and animals. (Kruse, 2006)

Table 1.1. Permeability and occurrence of human aquaporins. Modified from (Castle, 2005).

AQP	Permeants	Major tissue distribution
AQP0	↓ Water	Lens (eye)
AQP1	↑ Water CO_2; NO (Carbrey, 2009)	Erythrocytes, lung, kidney, brain, eye and vascular endothelium
AQP2	↑ Water	Kidney
AQP3	↑ Water ↑ glycerol; urea H_2O_2 (Miller, 2010)	Skin, kidney, lung, eye and GI tract
AQP4	↑ Water	Kidney, brain, lung, GI tract and muscle
AQP5	↑ Water	Salivary, lacrimal and sweat glands, lung and eye
AQP6	↓ Water Anions (NO_3^-> Cl^-) (Carbrey, 2009)	Kidney
AQP7	↑ Water ↑ glycerol; urea (Wspalz, 2009) Arsenite (Carbrey, 2009)	Adipose tissue, kidney and testis
AQP8	↑ Water urea; ammonia (Wspalz, 2009) H_2O_2 (Wu, 2007)	Kidney, liver, pancreas, GI tract and testis
AQP9	↓ Water ↑ glycerol; urea (Wspalz, 2009) Arsenite (Carbrey, 2009)	Liver, leukocytes, brain and testis
AQP10	↓ Water ↑ glycerol; urea (Wspalz, 2009)	GI tract
AQP11	NK	Brain, liver, kidney
AQP12	NK	Pancreas (Ishibashi, 2009)

NK – not known.

In humans, 13 different AQP isoforms are known (AQP0-AQP12) and they are classified into two different subgroups according to their ability to strictly transport water or also other small molecules such as glycerol: the orthodox aquaporins (AQP0, AQP1, AQP2, AQP4, AQP5, AQP6, AQP8) and the aquaglyceroporins (AQP3, AQP7, AQP9, AQP10). Additionally, AQP11 and AQP12 were found in intracellular membranes but their function is yet not defined. (Magni, 2006; Ishibashi, 2009)

Mammalian AQPs are organ, tissue and localization specific, being differentially expressed in epithelial tissues involved in fluid transport (e.g. epithelia from kidney and intestine) but also in other non-fluid transporting tissues such as skin, fat and brain. Table 1.1 shows the tissue distribution of AQPs in mammals.

1.1.1. Structure of aquaporins

AQPs are homotetrameric proteins (featuring four independent pores) with approximately 270 amino acids per monomer, each monomer behaving as a water channel. All AQPs share a similar structure (Figure 1.1) where, in general, each monomer comprises six membrane-spanning helical domains (H1-H6), organized in two distinct halves (H2, H1, H3 and H5, H4, H6) that interact to form a pore. These six highly hydrophobic transmembrane spanning helices are connected by five loops: three extracellular - loops A, C and E, and two intracellular – loops B and D. Both amino- and carboxyl- terminal ends are cytoplasmatic. Loops B and E present a consensus motif highly conserved, asparagine–proline–alanine (NPA; single letter code for amino acid) considered the channel signature and crucial for selectivity, namely the water/solute specificity.

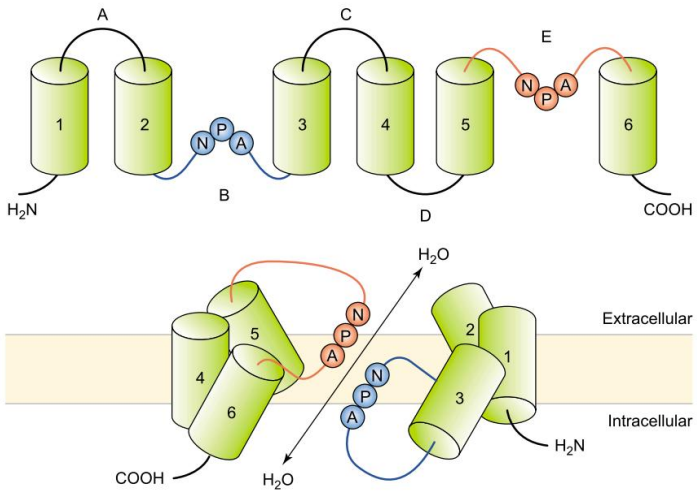

Figure 1.1. Structural organization of an AQP1 monomer. In the membrane, the six α helices form a right-handed twisted arrangement. However and to simplify, the helices 3, 1 and 2 are drawn separated from helices 5, 4 and 6. Adapted from (Zeuthen, 2001).

Loops B and E, which are shaped into small α helices as shown in Figure 1.2, fold back into the membrane and interact with the entire protein structure through hydrogen-bonds and several ion pairs. They also interact with each other by Van der Waal interactions between the proline residues of the NPA motifs. Thus, they are essential for the physiological role of AQPs in different ways: NPA motifs have both functional and positional relevance.

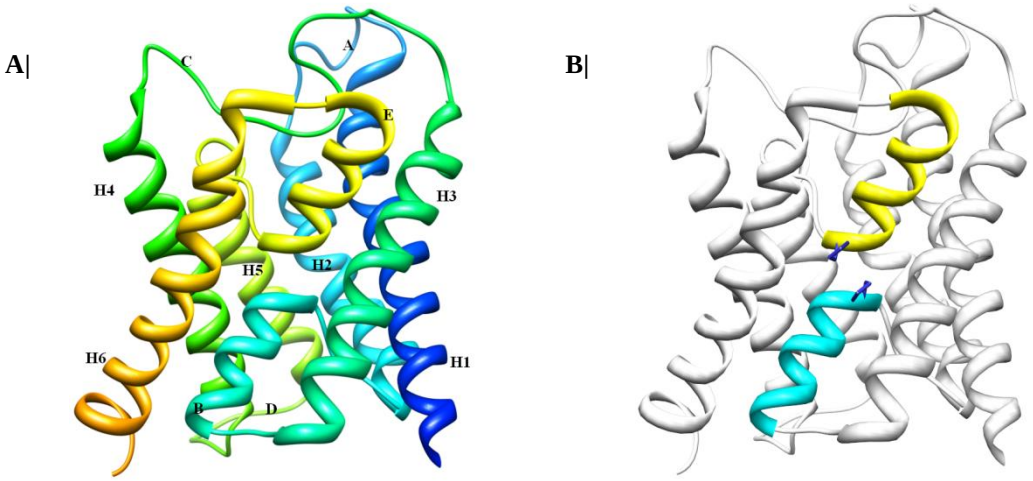

Figure 1.2. Representation of hAQP1 monomers (side view). Generated on *Chimera*. PDB ID: 1H6I**. A|** All the helices and loops are shown. **B|** Representation of loops B and E with the Proline residues of the NPA motif shown in dark blue.

Viewed from top of the extracellular surface, the six α helices form a right-handed, twisted arrangement. AQPs structure is achieved and maintained from the large crossing angles between helices, local fits between helices - ridges and grooves, and from interactions of highly conserved residues of Glycine at the crossing sites. (Zeuthen, 2001; Kruse, 2006)

1.1.2. Pore Structure of AQPs

Essential differences are found between aquaporins and aquaglyceroporins. In general, the pores of AQPs are roughly 25 Å long and exhibit two sites which interact strongly with water molecules: a constriction site and the NPA motif.

The first site of "selectivity" is located close to the relatively wide extracellular top of the pore: the diameter of this opening in orthodox aquaporins is approximately 2.8 Å, i.e. identical to that of a water molecule, while in aquaglyceroporins this opening is about 3.4 Å, matching the diameter of carbon hydroxyl groups of polyols such as glycerol. This constriction site is known as aromatic residue/arginine (ar/R) and is generally more hydrophobic in aquaglyceroporins.

The second interaction site is the NPA motif, the key for water/solute specificity. This region is larger than the ar/R, and it is located in the center of the pore (Figure 1.3). The small α helices at the end of loops B and E are capped with two polar uncharged amino-acids, two asparagines. These residues act like hydrogen donors to the oxygen atoms of the permeants. In addition, the water molecules that enter the pore are reoriented by the dipoles of the half helices (loops B and E), avoiding the formation of hydrogen bonds between adjacent water molecules. This dipole is also responsible for the exclusion of protons from the central region of the channel, through the free energy barrier that is generated.

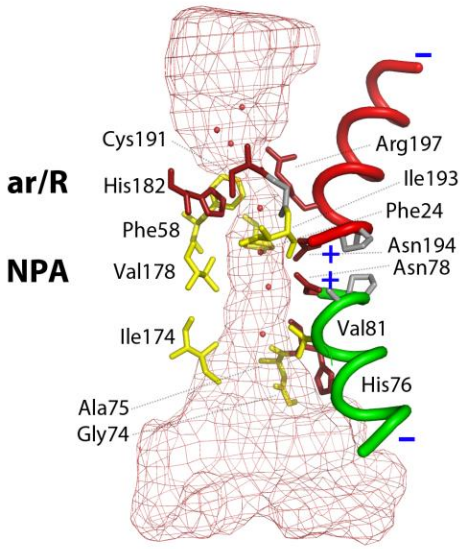

Figure 1.3. Detailed view of a bAQP1 (*bos taurus)* pore region (red mesh). Half helices dipoles and the hydrophilic and hydrophobic residues lining the pore are depicted in red and yellow, respectively. (Soveral G, 2011)

The NPA motif also confers size selectivity. In orthodox AQPs, the central region of the pore presents a leucine residue opposite to a phenylalanine (bulky side chain), while in aquaglyceroporins two leucine residues oppose to two asparagines. Thus, the pores of aquaglyceroporins are suitable for solutes larger than water.

The remaining residues, from the NPA to the intracellular top of the pore, exhibit hydrophobic side chains, with the carbonyls of the backbone exposed to the pore surface. The oxygen atoms, lined-up along one side of the pore, serve as hydrogen bond acceptors leading to an efficient transport of small hydrogen bond donors, such as water, urea or glycerol. (Wspalz, 2009)

Regarding the AQP gating, many factors are now known and well described, such as pH, osmotic stress, and even membrane tension or (de)activation through phosphorylation. (Soveral G, 2011)

1.2. AQP selectivity

1.2.1. Orthodox aquaporins

AQP1 is mainly found in erythrocytes and renal proximal tubules. (King, 2004) AQP1 water channels allow water to move freely and bidirectionally across the cell membrane, but exclude all ions including hydroxide, hydronium ions and protons, the later being essential to preserve the electrochemical potential across the membrane. It was recently described that AQP1 is also permeable to gases, such as carbon dioxide (CO_2) and nitric oxide (NO). However, the mechanism and the physiological relevance of this permeability (namely to CO_2) is still under debate and, thus far, this was the only AQP reported to be permeable to this gas. (Carbrey, 2009)

AQP0, AQP2, AQP4 and AQP5 are reported as strict water channels. (Takata, 2004)

AQP6 has been considered a special case, since it showed a low affinity for water (being only slightly permeable) but in contrast, is permeable to anions, namely nitrate and chloride. (Carbrey, 2009)

AQP8 is another particular case. Although with high affinity for water this channel also permeates hydrogen peroxide (Wu, 2007; Bertolotti, 2013) and was reported as a transporter for uncommon solutes such as ammonia derivates. (Liu, 2006)

1.2.2. Aquaglyceroporins

Aquaglyceroporins transport glycerol or other uncharged solutes in addition to water.

Compared with other mammalian orthodox aquaporins, namely with AQP1, AQP3 is moderately permeable to water, but highly permeable to glycerol and, possibly, to urea. Although unexpected, it was recently proposed to also act as a hydrogen peroxide channel, alongside with AQP8. (Miller, 2010; Bertolotti, 2013)

When expressed in *Xenopus* oocytes, the isoforms AQP7 and AQP10 were shown to transport water, glycerol and urea (Wspalz, 2009), while AQP9 was reported to transport all of these solutes plus a wide range of other solutes such as arsenite and antimonite. AQP7 is also permeable to these trivalent versions of the toxic metalloids, arsenic and antimony. (Carbrey, 2009)

1.3. Aquaporinopathies – AQP-related human diseases

AQPs are extensively expressed in human body and play several roles in different physiological processes, such as the urinary concentrating mechanism, glandular secretion or skin hydration. AQP0, for example, being exclusively expressed in the eye lens, plays a central role in maintaining lens transparency. This water channel constitutes 60% of lens membrane proteins and, when absent, leads to the development of cataracts in humans and mice. (Ishibashi, 2009)
Although there is still much to learn on the pathological processes arising from AQPs mutations or dysfunction, several unexpected pathologies have already been associated with/or attributed to the impaired function of water channels. Among them are brain edema, epilepsy, obesity, diabetes and cancer, where AQPs play unpredictable roles. (Verkman, 2009)

1.3.1. AQPs in cancer

Until 2008, twelve different tumor cell types in humans and mice were reported to express AQPs and for the majority, histological tumor grade showed a positive correlation with AQPs expression levels. (Verkman, 2008)
As shown in Table 1.2, several AQPs are found in different tumor types. Among them is AQP1, which is strongly expressed in tumor microvessels (Endo, 1999; Vacca, 2001), with an impressive presence in several cancers.

Table 1.2. AQP expression in different human tumors. Modified from (Verkman, 2008).

Tumor type	AQP	Expression
Glioma	AQP1, 3, 4, 5, 9	↑
Laryngeal cancer	AQP1	↑
Lung adenocarcinoma	AQP1, 3	↑
Renal cell	AQP1 AQP3	↓ ↑
Colorectal	AQP1,3,5 AQP8	↑ ↓

1.3.1.1. AQP-facilitated cellular migration

Studies with AQP1-null mice for investigation of a possible role of AQP1 in tumor angiogenesis, revealed a lower density of microvessels and consequently, an impaired angiogenic process. The overall result was a slowed tumor growth and improved survival. Other studies with AQP1-null mice reported a remarkable impairment in cellular migration, suggesting a strong correlation between AQP1 overexpression and migration. (Verkman, 2005) The same authors proposed a three step mechanism for AQP-facilitated cell migration, regardless of the cell type and AQP isoform (Verkman, 2008), as shown in Figure 1.4.

In the first step of cell migration, actin is cleaved leading to transient formation of membrane protrusions (lamellipodia and membrane ruffles). Ion uptake occurs at the tip of a lamellipodium (anterior end of the cell) creating local osmotic gradients. Consequently, a rapid water influx occurs increasing the local hydrostatic pressure, leading to the expansion of the cell membrane. If present, AQP polarizes to the leading edge of the cell membrane, facilitating water influx. Finally, actin repolymerizes leading to the stabilization of the protrusion. (Verkman, 2011a)

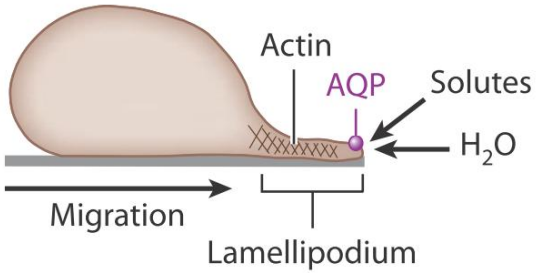

Figure 1.4. Proposed mechanism of AQP-facilitated cell migration. Water entry into protruding lamellipodia in migrating cells. Modified from (Verkman, 2012).

When expressed in tumor cells, AQP increases their ability to extravasate across blood vessels and to invade local tissues. (Hu, 2006) AQP-facilitated cell migration thus appears to be important not only in angiogenesis but also in tumor cell metastasis and spread. These findings may explain the high expression levels of AQPs in different tumor types and the correlation between AQP expression levels and tumor grade. (Verkman, 2012)

It must be noted that even non-orthodox AQPs are able to transport water.

1.3.1.2. AQP3 in skin tumorigenesis

AQP3 is an aquaglyceroporin widely expressed in many human tissues. Recently, analysis of AQP3-knockout mice has provided interesting information on the glycerol transport through this channel. In addition, different skin pathologies have been associated to AQP3 misexpression, namely skin cancer. (Hara-Chikuma, 2008a,b)

Mammalian skin is composed by three different layers, as shown in Figure 1.5A. The deepest layer of skin is rich in adipocytes. Above lies the dermis, rich in capillaries and composed by collagen fibers and elastin (among other components), that acts as a support layer for the third and most superficial skin layer, the epidermis. This region contains several different cell layers, being the external layer the stratum corneum (SC), that consists in terminally differentiated keratinocytes. These cells provide the outermost barrier against loss of body fluids. Thus, adequate hydration of the SC is essential for the maintenance of the skin health, allowing its flexibility and decreased vulnerability to external aggressions. (Rojek, 2008)
In mammalian skin, AQP3 is strongly expressed at the basal membrane of keratinocytes (Figure 1.5B). Studies with hairless mice lacking AQP3 exhibit reduced SC hydration (Verkman, 2005), reduced skin elasticity, delayed wound healing and delayed biosynthesis of SC (after removal by tape-stripping) (Hara, 2002). Studies using AQP3-null mice have also shown that water transport through AQP3 is not a rate-limiting factor in the trans-epidermal water loss. (Verkman, 2005)

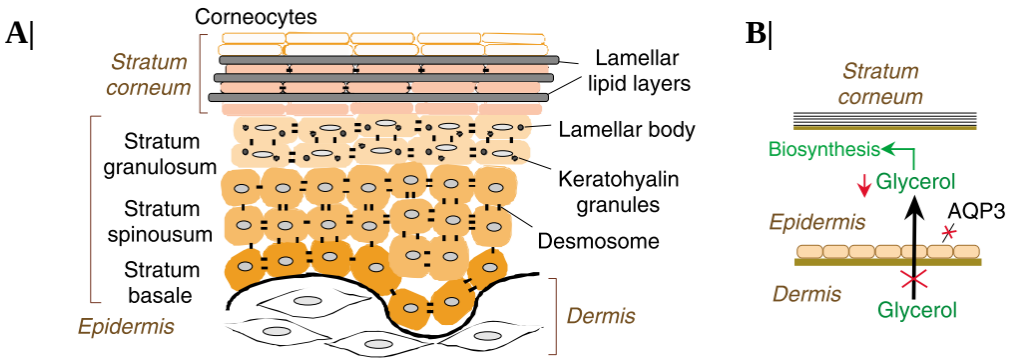

Figure 1.5. Reduced skin hydration in AQP3 deficiency. A| Schematic representaion of skin layers; **B|** Proposed mechanism of AQP3 function in the skin. Modified from (Verkman, 2005).

The AQP3 deficiency in the skin reflects reduced epidermal glycerol permeability and reduced glycerol content in SC and epidermis, while normal glycerol content in serum and dermis. Thus, a reduced glycerol transport from blood into the epidermis, through the basal keratinocytes, is pointed as the plausible responsible for the skin phenotype in AQP3-null mice. (Verkman, 2005)

More recently, studies in mice with disrupted AQP3 gene, revealed reduced epidermal pools of glycerol, glucose and ATP. (Hara-Chikuma, 2008b) Hara-Chikuma and co-workers also found a positive correlation between glycerol and ATP content in AQP3$^{+/+}$ mice keratinocytes, suggesting the involvement of AQP3-mediated glycerol transport in ATP synthesis. This fact, together with a positive correlation between ATP content and cell proliferation, brought new clues about the importance of AQP3 in states of epidermal hyperproliferation, such as psoriasis, atopic dermatitis, wound healing, ichthyosis and even tumorigenisis, where it is upregulated. Summarizing, AQP3 plays central roles in skin hydration, wound healing and tumorigenesis (Hara-Chikuma, 2008b,c) although the implicit mechanism of tumorigenesis resistance observed for AQP3-null phenotype is still not clear. Figure 1.6 illustrates the proposed pathways for AQP3-dependent skin hydration, wound healing and AQP3-dependent cell proliferation during skin tumorigenisis. According to this mechanism, the overexpression of AQP3 leads to an increased glycerol uptake. As a rich energetic substrate, a high glycerol pool leads to increased ATP synthesis and, consequently, cell proliferation. Notwithstanding, and regarding AQP3 in particular, the triggering pathway for tumorigenesis is still obscure.

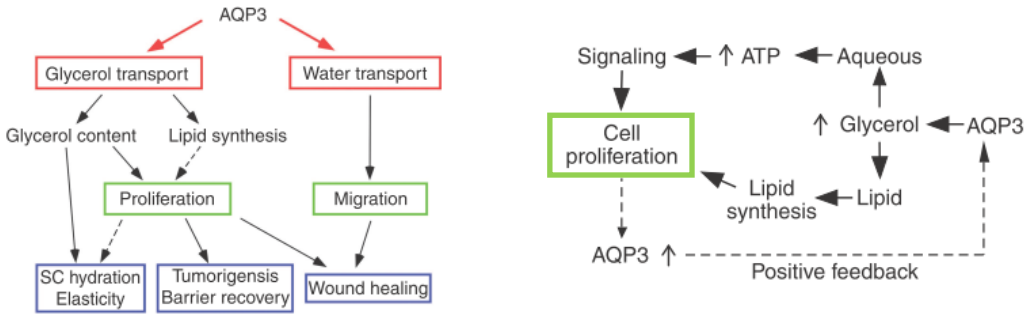

Figure 1.6. Schematic representation of the proposed mechanisms of AQP3-dependent skin hydration, wound healing, and tumorigenesis. Modified from (Hara-Chikuma, 2008c; Verkman, 2009).

It must be noted that in 2012, Gao and co-workers described the contribution of AQP3 to the chemoresistance of melanoma to arsenite. (Gao, 2012) In addition, other studies identified an unexpected permeant for AQP3, the hydrogen peroxide (Miller, 2010; Bertolotti, 2013). This fact may unravel new unexpected roles for AQP3 in tumor biology through oxidative stress.

(For recent reviews of the roles of AQPs in Medicine *see*: (Verkman, 2012,2013))

1.4. AQP inhibitors: pharmaceutical opportunities

Several pathologies have been associated and/or attributed to the impaired functioning of AQPs. Consequently, the potential utility of aquaporin modulators for the treatment of several pathologies such as kidney diseases, obesity, glaucoma, brain edema, epilepsy and cancer should be considered. (Verkman, 2009)

As an example, AQP1-null xenograft models of subcutaneous melanoma tumors showed decreased tumor growth and reduced angiogenesis when compared to wild-type controls. These observations were associated with AQP1 gene disruption. (Lopez-Campos, 2011; Machida, 2011) Moreover, a chemical down-regulation of AQP1 expression was reported to block angiogenesis and tumor growth. (Bin, 2011)

Due to the central roles of AQP3 in epidermal cell migration and proliferation (Hara-Chikuma, 2008b,c) this aquaglyceroporin can also be seen as a potential target for cancer therapy. Recently, AQP3 inhibition by copper(II) ions reduced cell growth rates and increased the therapeutic efficacy of Cisplatin. (Huber, 2012)

Therefore, pharmacotherapy via AQP modulation should be considered as a valuable strategy for treating several and different human diseases. Despite AQP-based therapy for human diseases still being considered a distant reality, recent progresses were achieved with AQP4 in neuromyelitis optica. (Verkman, 2011b; Huber, 2012)

1.4.1. Metal-based agents as AQP3 inhibitors

Recently, gold complexes were described as new potent inhibitors of AQP3, being four times more effective, for the same concentration, than the common mercurial compounds used for AQP inhibition studies *in vitro*. (Martins, 2012)

In 2012, Martins and co-workers reported $[Au(phen)Cl_2]Cl$ (phen= phenantroline, Auphen) and $[Au(dien)Cl]Cl_2$ (dien= diethylendiamine, Audien) as potent and highly selective inhibitors of the glycerol transport in human RBCs (90% inhibition) with half-inhibitory concentration (IC_{50}) values in the low-micromolar range. In addition, these Au(III) compounds showed to be non-toxic in RBC during the time span of channel inhibition. Their water solubility, plus the previous considerations, makes them suitable drugs for *in vivo* studies. (Martins, 2012) More recently, the same group tested other Au(III) compounds as AQP3 inhibitors. In order to evaluate and compare the influence of metal substitution on the inhibitory potency, the Cu(II) compound Cuphen was also tested.

As result, the following compounds were also identified as potent and selective AQP3 inhibitors: $[Cu(phen)Cl_2]Cl$ (phen= phenantroline, Cuphen), $[Au(terpy)Cl]Cl_2$ (terpy = terpyridine, Auterpy), $[Au(bipy(R,R'))Cl_2]PF_6$ (bipy = bipyridyl) where R=R'= H, Me, NH_2 (Aubipy, AubipyMe, $AubipyNH_2$ respectively). (Martins, 2013)

Figure 1.7 displays the structures of several metallodrugs described as AQP3 inhibitors.

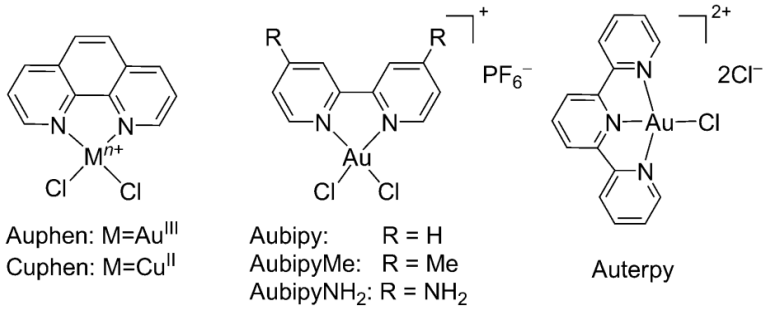

Figure 1.7. Structures of several metallodrugs described as AQP3 inhibitors by Martins and colleagues. Modified from (Martins, 2013).

At this point, it is interesting to refer that all of these gold complexes were already described as antiproliferative agents *in vitro*, being considered as promising candidates to anticancer drugs. (Messori, 2000; Casini, 2009; Serratrice, 2012)

1.4.2. Metallodrugs as antitumoral agents

Metal compounds have been widely used in medicine for several decades. Among them we can find bismuth (anti-ulcer), silver (anti-microbial) and iron (anti-malarial) compounds and, in terms of anti-tumor activity, the earliest reports date from the sixteenth century. (Desoize, 2004)

In the 1960s, B. Rosenberg discovered a platinum-based compound – cisplatin - with antitumor activity (Rosenberg, 1965, 1969), which became approved by the FDA in 1978 and still continues to be the first line of treatment for some types of cancer. (Guidi, 2012) Thus, metallodrugs are still a promising research area, drawing increased attention within the medicinal chemistry communities due to their antiproliferative and antitumor properties, obtained in both *in vitro* and *in vivo* studies. (Nobili, 2010; Berners-Price, 2011)

Since 1890, when Robert Koch discovered that gold cyanide was able to inhibit the growth of *M. tuberculosis,* gold compounds started to be developed as therapeutic agents. (Benedek, 2004)

In the mid 1980s, auranofin, an orally active Au(I) which was approved for rheumatoid arthritis treatment, was described as an inhibitor of tumor cells growth *in vitro.* (Mirabelli, 1985)

This was the beginning of a great advance in medicinal inorganic chemistry and metal-based compounds started to gain relevance in this field. This fact is due to the variety of properties that metal-based compounds can present like the coordination number, redox state or different geometries in addition to the intrinsic properties of the metal ion itself, dictating alterations in the compound reactivity.

By this time, Cisplatin was already marketed and Au(III) compounds, with square planar geometry, were seen as possible mimetics, since they present the same electronic configuration.

The AQP3 inhibitors described above, including the Au(III), are examples of metallodrugs with cytotoxic activity. It is important to highlight that several Au(III) compounds are already described as being more potent than Cisplatin, overcoming the recurrent resistance problems associated to this chemotherapeutic. (Messori, 2000)

Despite the cytotoxic potential presented by metallodrugs, and in particular Au(III) compounds, this type of compounds have some drawbacks, namely instability under physiological conditions. As reactive molecules, they present high hydrolysis rates and reduction potential giving rise to the need of an adequate stabilization of these drugs at oxidation state +3. (Messori, 2004)

Several efforts have been made in order to synthesize gold complexes with increased stability under physiological conditions for pursuing Au(III) potential in cancer therapy. One approach consists on the stabilization of the metal center by nitrogen donors, to which Au(III) shows preference. Examples are Auphen and Auterpy (*see* Figure 1.7). (Nobili, 2010) Regarding Au(III) reactivity, it is also important to consider the variety of biological targets that this class of compounds may have *in vivo*. Human RBCs, in which glycerol movement across membranes is mostly mediated by AQP3, constitute a good example. (Martins, 2013)

In order to minimize the drawbacks mentioned above (i.e. drug instability and reactivity) appropriate carriers must be designed. In addition to a possible protection of the drug from inactivating events *in vivo*, an ideal carrier, among other characteristics, should be biocompatible and improve the therapeutic index of the associated compound.

1.5. Drug Delivery Systems (DDS)

For the last decades, several efforts have been made pursuing the improvement on pharmacokinetic, biodistribution and pharmacodynamic profiles of drug candidates, which in the free form, present pharmaceutical properties far from the ideal.

As briefly referred above, a drug carrier should provide the release of the drug within the therapeutic window at the site of action, must be biodegradable and/or easily excreted after exerting its therapeutic effect, should present low immunogenicity and prevent premature degradation of the drug. Ideally, it should also be stable upon storage and present low production costs. (Gaspar, 2008)

Regarding cancer therapy, and particularly solid tumors, the DDS should also provide the ability to penetrate into the tumor interstial space. Based on these previous considerations, the reason of nanotechnology growth in the recent years is evident. Within this area, and gathering all the properties of an ideal DDS, liposomes are considered one of the most promising and successful drug carriers for cancer therapy. (Allen, 2004)

1.5.1. Liposomes

Liposomes were described for the first time by Dr Alec D. Bangham roughly 50 years ago. (Bangham, 1965) These systems were firstly developed as models of biological membranes due to their architecture that mimics the molecular structure of natural cell membranes. As an example, the identification of the first AQP was performed after protein reconstitution into liposomes in 1992. (Zeidel, 1992)

In the 70's, these lipid systems started to be used for drug delivery (Gregoriadis, 1972) and nowadays, several liposomal formulations are already available in the clinic or in advanced development stages, for treatment of different pathologies including cancer. (Slingerland, 2012)

These vesicles may present mean sizes ranging from few nanometers (50 nm) to more than 1 μm, and are colloidal particles generally constituted by naturally occurring phospholipids and cholesterol, conferring biodegradability properties. These spherical vesicles are organized in bilayers, separated by aqueous compartments, mimicking cellular membranes, and possessing the ability to incorporate different substances/compounds independently of their properties such as molecular weight, solubility or charge. (Cruz, 2009)

Due to the liposomes typical structure, they are able to encapsulate/incorporate molecules with distinct properties, which is an advantage *per se*. Hydrophilic molecules can be entrapped in the aqueous compartments while compounds with hydrophobic properties can be partial or totally accommodated within the lipid bilayers, as shown in Figure 1.8A. (Bei, 2010)

Liposomes can be designed aiming therapeutic, diagnostic and even imaging purposes.

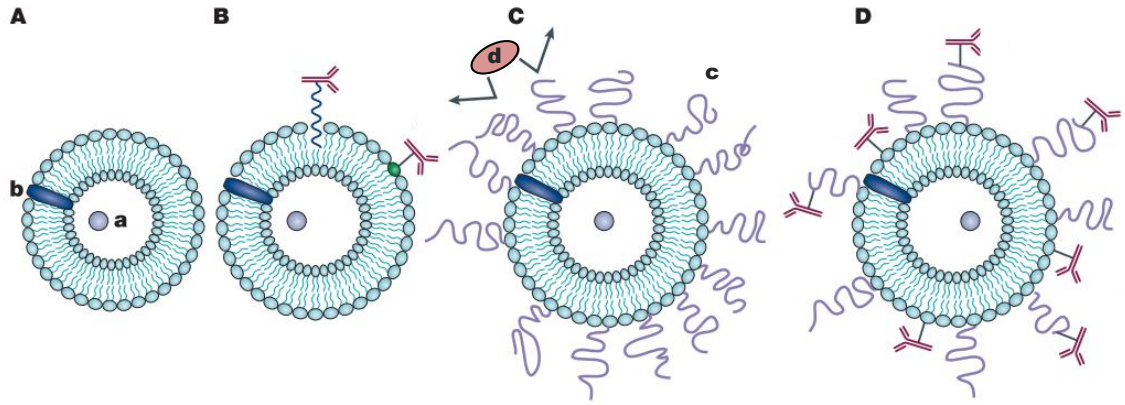

Figure 1.8. Liposomes – versatile structures. A| classic liposomes with hydrophilic drug **(a)** at the inner aqueous compartment and hydrophobic drug **(b)** within the lipid bilayer. **B|** Immunoliposomes possess specific antibodies (or antibody fragments) at surface to enhance a specific targeting. **C|** Long-circulating liposomes present modified surface by the presence of polymers such as PEG **(c)** that allows the increase of circulation time in bloodstream and protects the carrier from opsonizing proteins **(d)**. **D|** Long-circulating immunoliposome. Adapted from (Torchilin, 2005).

Focusing on their therapeutic action, liposomes as DDS present several advantages over non-encapsulated drugs.

In addition to the fact that liposomes are able to entrap a therapeutic molecule in their structure, several other advantages should also be mentioned. Liposomes are able to enhance drug solubility and to protect the incorporated drug from premature degradation or metabolization, while keeping its therapeutic activity, affording to a partial reduction of possible side-effects in healthy tissues and/or organs. Moreover, liposomes present a high versatility. They can be constructed according to the physicochemical properties of each particular drug or to the desired target tissue or organ. This may be performed by i) varying the lipidic constituents, ii) changing bilayer rigidity, iii) adding surfactants to lipid composition to alter superficial charge and, consequently, their stability and/or interaction with affected cells or organs, iv) attaching different polymers as shown in Figure 1.8C (such as PEG) to enhance the half-time of the vesicle in bloodstream and, consequently, of the drug and even iv) including antibodies or antibody fragments at the liposome surface for a specific targeting, as shown in Figure 1.8B and D. (Torchilin, 2005, 2007; Cruz, 2009)

From all above mentioned advantages, the most important strength of these systems is their ability to improve pharmacokinetics (PK) and biodistribution (BD) of the associated therapeutics. Liposomes, depending on their lipid constituents, are able to increase the circulation in the bloodstream of the incorporated drug reducing its clearance. This type of lipid vesicles is designed as long-circulating liposomes (LCL) and they may be constructed by inclusion in the lipid composition of different polymers, covalently linked to phospholipids. Polyethylene glycol (PEG) is the most popular polymer used. (Harris, 2003) The presence of PEG at liposome surface, as shown in Figure 1.8C, reduces the adsorption of plasma proteins. Due to these characteristics, this type of liposomes, after parenteral administration, is able to have a longer circulation time in bloodstream. Regarding BD, alterations can occur via the so called enhanced permeability and retention (EPR) effect, also called passive targeting. (Maeda, 2000, 2001) Several pathological conditions present increased permeability of tissue vasculature. Solid tumors are a good example of compromised vasculature. As tumor tissue starts to grow, the support of nutrients and oxygen will eventually be insufficient for tumor nutritional requirements. To overcome this situation, cytokines and other signaling molecules are released from tumor cells in order to recruit more blood vessels in a process called angiogenesis. Angiogenic blood vessels present gaps of 600 to 800 nm between adjacent endothelial cells (Figure 1.9) allowing the extravasation of liposomes to the interstitial space in a size-dependent manner.

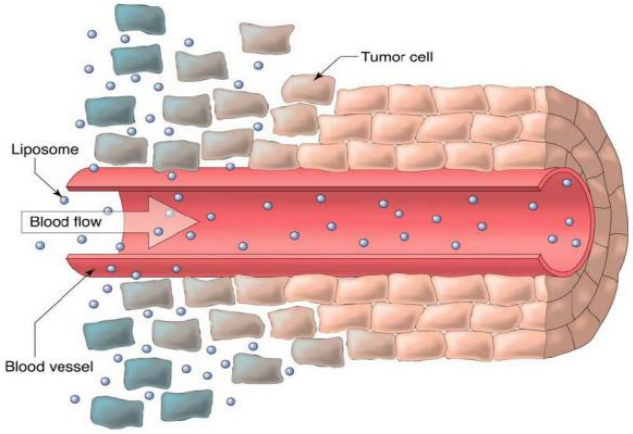

Figure 1.9. Extravasation and accumulation of liposomes in tumor tissue due to EPR effect. (Saetern, 2004)

As these lipid systems present sizes substantially lower, they tend to accumulate in the tumor tissue. Thus, to take advantage of this EPR effect, liposomes must present long circulation times in the bloodstream (by the inclusion of PEG in lipid composition, for example) in order to enable, to a higher extent, the extravasation of the drug into the tumor.

In addition to the preferential targeting of liposomes to tumor vasculature, it is important to refer that, in general, tumor tissues lack an effective lymphatic drainage. Therefore, extravasated liposomes are able to accumulate in tumor tissues. (Allen, 2004; Torchilin, 2007; Cruz, 2009)

All of these characteristics, combined with the already mentioned biodegradability, make liposomes a suitable and promising carrier for clinical use and, particularly, for cancer therapy.

1.6. Aims and goals

In the present study the first objective was to validate the cytotoxicity of a small library of metallodrugs, already described as AQP3 inhibitors. Based on the cytotoxic screening, one compound was selected to be further incorporated in an adequate delivery system, liposomes. The second objective of the work was the design and development of liposomal formulations able to incorporate the selected compound. The third objective was the *in vitro* evaluation of the cytotoxic activity of the AQP3 inhibitor previously selected, both in the free and in the liposomal forms, in two cancer cell lines.

In order to fulfill the objectives of the present thesis the work was persecuted according to the following:

1. Validation of cytotoxicity of a small library of metallodrugs already described as AQP3 inhibitors against a human epidermoid carcinoma cell line (A431) overexpressing this aquaglyceroporin;
2. Selection of a single compound to be incorporated in liposomes, based on the cytotoxic activity against A431 cells;
3. Establishment of an adequate methodology for quantification of the selected AQP3 inhibitor;
4. Development and characterization of liposomes incorporating the AQP3 inhibitor. In particular, the influence of lipid composition, mean size and superficial charge on incorporation parameters were studied;
5. Cytotoxic *in vitro* studies of the selected metallodrug formulations in free and liposomal forms against two cancer cell lines: the A431 and the murine colon cancer cell line, C26.

It is important to highlight that, due to similarities of the metallodrugs tested, the developed formulation can be seen as a model for further studies involving other AQP3 inhibitors.

2. Materials and Methods

2.1. Materials

All the metallodrugs were synthesized and gently provided by Dr. Angela Casini (Pharmacokinetics, Toxicology and Targeting, Research Institute of Pharmacy, University of Groningen).

Six mononuclear compounds were included in the present work: $[Au(phen)Cl_2]Cl$ (phen=1,10-phenantroline, Auphen), $[Cu(phen)Cl_2]Cl$ (Cuphen) $[Au(dien)Cl]Cl_2$ (dien = diethylentriamine, Audien), $[Au(terpy)Cl]Cl_2$ (terpy = tripyridine) and two different compounds based on the following $[Au(bipy(R,R'))Cl_2]PF_6$ (bipy = 2,2'-bipyridine, Aubipy), where R=R'= H, or Me. Aubipy compounds will be referred according to the substituent group:. R=Me, AubipyMe, R=H, Aubipy.

The pure phospholipids, egg phosphatidylcholine (PC), dimyristoyl phosphatidylcholine (DMPC), Dipalmitoyl phosphatidylcholine (DPPC) and distearoyl phosphatidylethanolamine covalently linked to poly(ethylene glycol) 2000 (PEG), used for the preparation of liposomal formulations were purchased from Avanti Polar Lipids (Alabaster, AL).
Deionized water (Milli-Q system; Millipore, Tokio) was used in all experiments. Nuclepore Track-Etch Membranes were purchased from Whatman Ltd, (NY, USA). Culture media and antibiotics were obtained from Invitrogen (Life Technologies Corporation, NY, USA). Reagents for cell proliferation assays were purchased from Promega, (Madison, WI, USA). Octadecylamine (n-Stearylamine (SA)), cholesterol (Chol) and Hoescht 33258 were purchased from Sigma (Sigma-Aldrich, St. Louis, MO, USA). All the remaining chemicals and substrates used were of analytical grade.

2.2. Methods

2.2.1. Preparation of Cuphen liposomal formulations

Liposomes composed of the selected phospholipids were prepared by the dehydration-rehydration method (DRV) (Cruz, 1993; Gaspar, 1996, 2008). Briefly, the selected phospholipids (20µmol/mL) were dissolved in chloroform and the mixture was dried by rotary evaporation (Buchi, Switzerland) of the organic solvent to obtain a thin film in a round-bottom flask. The film was then dispersed in a Cuphen solution, frozen (-70ºC) and lyophilized (Freeze dryer, Edwards, USA) overnight.

The rehydration of the lyophilized powder was performed with a buffer constituted of 10 mM HEPES and 145 mM NaCl, pH 7.4 (HEPES buffer) in two steps, in order to enhance the Cuphen incorporation (Lasch, 2003): first, a 30 minute step where two-tenth of the original dispersion was added, and subsequently, the addition of the remaining volume (up to the starting volume). Here it is important to refer that the hydration steps should always be performed at a temperature above the phase transition temperature (Tc) of the phospholipids.

In order to reduce and homogenize the mean size of liposomes, the so formed vesicles were submitted to an extrusion step through polycarbonate membranes of appropriate pore size until the desired vesicle size is reached (1, 0.8, 0.6, 0.4 (3x), 0.2 (3x) and 0.1 (3x) µm) under nitrogen pressure (10-500 lb/in^2) with an Extruder device (Lipex: Biomembranes Inc., Vancouver, British Columbia, Canada).

The separation of non incorporated Cuphen was performed by ultracentrifugation at 250,000 g for 120 min at 15ºC in a Beckman LM-80 ultracentrifuge (Beckman Instruments, Inc, USA.) Finally, the pellet was ressuspended in HEPES buffer, according to the final concentration desired.

2.2.2. Characterization of Cuphen liposomal formulations

Liposomes were characterized in terms of lipid composition, lipid (Lip) and Cuphen concentration, mean diameter, zeta potential and by the following incorporation parameters: initial and final Cuphen to lipid ratios [(Cuphen/Lip)i and (Cuphen/Lip)f, respectively] and incorporation efficiency (I.E.) defined as the percentage of [(Cuphen/Lip)f]/[(Cuphen/Lip)i].

The I.E., being a ratio between final to initial (Cuphen/Lip), determines the ability that a particular lipid mixture presents for incorporating Cuphen in liposomal matrix.

2.2.2.1. Cuphen quantification

UV/Vis spectroscopy, due to its simplicity and reliability was the selected technique for Cuphen quantification. Moreover, the destruction of liposomes was performed by addition of absolute ethanol (EtOH).

From a stock solution of 200nmol/mL in EtOH, serial dilutions were performed with the same organic solvent and UV spectra were traced (220nm-800nm) in a UV/Vis spectrophotometer (Shimadzu UV 160A).

After selection of the appropriate wavelength, calibration curves were performed in order to evaluate the relation between the absorbance values and concentration. The selected concentrations ranged from 2 μM up to 20 μM, in order to ensure linearity and enabling the determination of Cuphen content in developed formulations after liposome disruption with EtOH.

2.2.2.2. Phospholipid quantification

The method for phospholipid quantification was based on the colorimetric determination of phosphate (PO_4^{-3}). In the presence of ammonium heptamolybdate ($(NH_4)_6Mo_7O_{24}.4H_2O$) the inorganic phosphate was converted to phosphomolybdic acid, which was quantitatively converted to a blue color due to reduction of ascorbic acid during heating, using the method described by Rouser and co-workers (Rouser, 1970). Briefly, samples (in triplicate) containing phosphate quantities between 20 and 80 nmol (sample volume below 100 μL) were pipetted into 15 mL glass tubes. In parallel, a calibration curve from a 0.5 mM phosphate solution was prepared: in triplicate, phosphate amounts of 20, 30, 40, 50, 60 and 80 nmol were pipetted into glass tubes. All tubes were heated (180ºC) in a heating block until dryness. After cooling, 0.3 mL of perchloric acid (70-72%) was added to all tubes. In order to avoid volume losses, marbles were placed on the top of all glass tubes. At this point, all tubes were heated in the heating block (180ºC) for 45 min, to convert all the organic lipid phosphate to the inorganic form and until achievement of a clear solution. After cooling samples to room temperature, 1.0 mL of H_2O, 0.4 mL of hexa ammonium heptamolybdate solution [1.25% (w/v)] followed by 0.4 mL of ascorbic acid solution [5% (w/v)] were added to all glass tubes. A blue color solution was obtained due to the reduction of ascorbic acid during heating in a boiling water bath for 5 min. After cooling, the absorbance of all samples was recorded (797nm) in a UV-mini 1240 Spectrophotometer (Shimadzu). The amount of phosphate in samples was obtained through the calibration curve with the aid of linear regression. The calibration curve was linear up to absorbance values of around 1.000.

2.2.2.3. Liposome size measurements

Liposome mean diameter was determined by dynamic light scattering based on Brownian motion of the particles in a hydrodynamic sizing system (Zetasizer Nano S (Zen 1600), Malvern Instruments, UK). For viscosity and refractive index, the values of pure water were used. As a measure of particle size distribution of the dispersion, the system reports the polydispersity index, (P.I.). P.I. ranges from 0.0, for an entirely monodisperse sample, up to 1.0 for a polydisperse suspension. To determine the mean diameter and P.I. of liposomal preparations, samples were diluted to a final lipid concentration of 0.2 µmol/mL in HEPES buffer. All the measurements were done in an appropriate polycarbonate cell at a temperature of 25ºC.

All liposomal formulations were prepared in order to obtain a P.I. < 0.30.
To ensure that appropriate mean diameter and P.I. were achieved, these parameters were also determined during the extrusion procedure.

2.2.2.4. Zeta potential determination

Zeta potential of liposomal formulations was measured in a hydrodynamic sizing system (Zetasizer Nano Z (Zen 2600), Malvern Instruments, UK). Zeta potential is defined as an electric potential between the membrane surface and the ionic dispersion medium. Zeta potential was measured using a combination of the measurement techniques: Electrophoresis and Laser Doppler Velocimetry, sometimes called Laser Doppler Electrophoresis. This method measures how fast a particle moves in a liquid when an electrical field is applied. For viscosity and refractive index, the values of pure water were used.
Before determination of the zeta potential of liposomal formulations, an initial check of the apparatus was made with a standard known zeta potential value (standard DTS5050, Malvern Instruments, Ltd., UK). Dilutions of liposomal formulations were made in HEPES buffer, at a final lipid concentration of about 0.2 µmol/mL. Samples were slowly introduced into a clear disposable zeta cell with a syringe to avoid air bubbles. The zeta potential of samples was recorded at a temperature of 25ºC.

2.2.2.5. Stability of Cuphen liposomes

The stability in suspension of Cuphen liposomes was assessed by quantifying Cuphen and lipid contents after storage at 4ºC for 10 days.

After this storage period (t=10), samples were taken (t=0), diluted in HEPES buffer and submitted to a centrifugation step (250,000 g for 120 min at 15ºC). Liposomes were ressuspended in HEPES buffer according to the initial volume. Cuphen and phospholipid contents were quantified. The stability was defined as the ratio in percentage between Cuphen to lipid ratio at t=10 and the initial Cuphen to lipid ratio at zero time (t=0), according to the following formula: $[(Cuphen/Lip)_{t=10}/(Cuphen/Lip)_{t=0}] \times 100$.

In addition, vesicles mean size and zeta potential were also determined.

2.2.3. Cell Culture

Human epidermoid carcinoma cells, A431, gently provided by Prof. Eschevarria (Instituto de Biomedicina de Sevilla (IBIS), Hospital Universitario Virgen del Rocío, Seville, Spain) were seeded in culture flasks and maintained in Dulbecco's modified Eagle's medium (DMEM) with high-glucose (4500 mg/L), supplemented with 10% fetal bovine serum (FBS) and 100 µg/mL penicillin/streptomycin. Murine colon cancer cells, C26, obtained from CLS (Cell Lines Service, Life Technologies) were plated in culture flasks and maintained in Roswell Park Memorial Institute (RPMI) 1640 with the supplementation described above. Both cell lines were kept at 37° C under a 5% CO_2 atmosphere. Maintenance of cultures was performed every two/three days, until cells reached a confluence of about 80%. At this point, sub-culturing was performed using a solution of TrypLE (Invitrogen, Life Technologies Corporation, NY, USA). Briefly, after media removal, the cell layer was washed with phosphate buffered saline (PBS) and incubated with TrypLE for 7-10 minutes at 37ºC. After cells detachment, complete growth medium was added. The cells were then centrifuged in a bench centrifuge (Beckman, Izasa, Spain) at 500g for 10 min and the pellet ressuspended in fresh culture medium. Appropriate aliquots of the cell suspension were seeded in new culture flasks.

Cell storage was done in liquid nitrogen, in cryotubes with freezing medium consisting of FBS and 10% dimethylsulfoxide (DMSO).

2.2.4. Evaluation of cellular viability

2.2.4.1. Hoechst Staining

Hoechst labeling of attached cells stains chromatin and can be used to detect apoptotic nuclei by morphological analysis.

A431 cells were seeded (10^5 cells/mL) in 35mm dishes and incubated with 5, 15 and 50 μM of each of the gold compounds – Auphen, Auterpy, Audien, Aubipy and AubipyMe, for 24 and 48h. At each time point, culture medium was gently removed to prevent detachment of cells. Attached cells were fixed with 4 % paraformaldehyde in PBS, pH 7.4, for 10 min at room temperature, washed with PBS, incubated with Hoechst dye 33258 (Sigma-Aldrich Corp.) at 5 μg/mL in PBS for 5 min, washed with PBS, and mounted using Fluoromount-GTM (SouthernBiotech, Birmingham, AL, USA). Fluorescence was visualized using an Axioskop fluorescence microscope (Carl Zeiss GmbH, Jena, Germany). Blue-fluorescent nuclei were scored blindly and categorized according to the condensation and staining characteristics of chromatin. Normal nuclei showed non-condensed chromatin disperse over the entire nucleus. Apoptotic nuclei were identified by condensed chromatin, contiguous to the nuclear membrane, as well as by nuclear fragmentation of condensed chromatin. Five random microscopic fields per sample of approximately 150 nuclei were counted and mean values expressed as the percentage of apoptotic nuclei.

2.2.4.2. Trypan Blue assay

The trypan blue exclusion method was used to evaluate total cell death. Trypan blue is a cell stain that only permeates non-viable cells; i.e. cells whose permeability is somehow compromised.

This assay was performed in parallel with the Hoechst staining: briefly, the media/supernatant was removed from 35mm dishes and centrifuged at 600g for 4 minutes. The cell pellet was ressuspended in 10μL of Trypan Blue 0.4%. Dead cells (stained) were counted under a brightfield microscopy (Carl Zeiss GmbH, Hamburg, Germany).

2.2.5. MTS assay

CellTiter 96®AQueous Non-Radioactive Cell Proliferation Assay (Promega, Madison, USA) is a ready-to-use mix of substrates which allows the measurement of the metabolic activity of viable cells by reduction of a tetrazolium salt. Briefly, dehydrogenase enzymes found in

metabolically active cells convert the tetrazolium compound (inner salt; MTS) to a water soluble formazan dye, which can be quantified spectrophotometrically - absorbance measured at 490nm and directly correlated to viable cells number. (Cory, 1991; Riss, 1992). The assay was performed according to manufacturer's instructions.

2.2.5.1. Metallodrugs cytotoxicity screening

Briefly, A431 cells were seeded in 96-well plates (100 µL; 10^5 cells/mL) for 24h. Stock solutions of metallodrugs were prepared in Milli-Q water. Cells were incubated with each metallodrug at concentrations ranging from 0.25 µM to 60µM for 48h and 72h. All the experiments were performed in triplicate. At each timepoint, the media was removed and replaced with fresh media. Subsequently, 20 µL of MTS were added to each well, plates slightly agitated and incubated, under the same culture conditions mentioned above. Absorbance was measured 60, 90 and 120 min after MTS addition, at 490nm in a BioRad microplate reader Model 680 (Bio-Rad, Hercules, CA).

2.2.5.2. Cytotoxic effect of Cuphen formulations against cancer cells

For these procedures, a Cuphen stock solution of 500nmol/mL was prepared in PBS and filtered through a sterile syringe filter (0.20 µm). From the stock solution, different dilutions were performed with the respective culture medium according to the desired concentrations for each experiment.

For the determination of the cytotoxic effects of free and liposomal Cuphen, 7.5 x 10^4 cells/mL were used for both A431 and C26 cells. (Calado, 2012)
Cells were plated in 96-well plates (200 µL) under the culture conditions described above (*see* 2.2.3 Cell Culture). Twenty-four hours after plating, medium was removed and adherent cells were treated with Cuphen in the free or in the liposomal form, with concentrations ranging from 0.625 µM to 50 µM (100 µL of the respective dilution per well). Three different incubation periods were tested (48h, 72h and 96h).
Negative control was constituted by the cell line under study in the presence of the culture medium. Unloaded liposomes also constituted another control group, using the same lipid concentrations as in loaded liposomes.

All tests were performed with six samples for each concentration under study.

2.2.6. Statistical analysis

All data presented are expressed as mean ± standard deviation (S.D.) with the exception of the cytotoxicity results (i.e. IC_{50} values). For this last case, data is presented as the best fit value ± standard error (S.E.). Statistical analysis was performed using the ANOVA One Single Factor. The acceptable probability for a significant difference between mean values was $p<0.05$.

3. Results and Discussion

3.1. Metallodrugs cytotoxicity screening

In order to select a unique metallodrug for incorporation into liposomes, trypan blue assay, Hoechst staining and the MTS assay were performed with a small library of metallodrugs, previously described as AQP3 inhibitors, using the A431 human epidermoid carcinoma cell line.

3.1.1. Trypan Blue assay and Hoechst staining

A431 cells were incubated with Auphen, Auterpy, Audien, Aubipy or AubipyMe for 24h (Figure 3.1) and 48h at different concentrations (5, 15 and 50 μM) and cell death analyzed using the trypan blue assay.

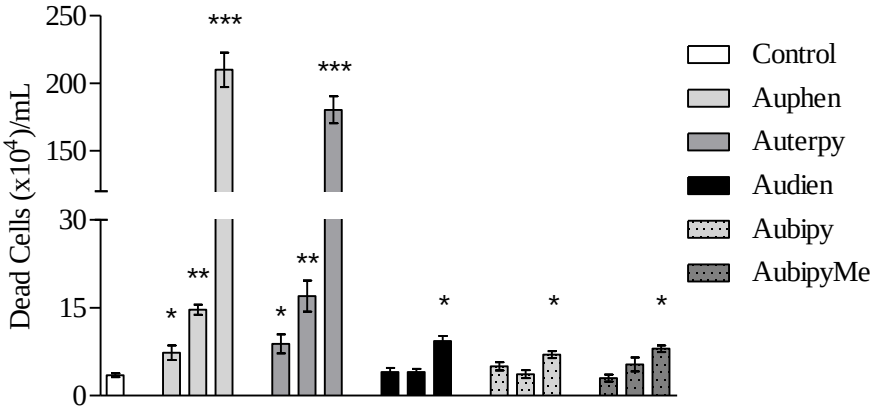

Figure 3.1. Cellular death induced by the different AQP3 inhibitors at 5, 15 and 50 μM (shown in ascending order), after incubation in A431 cells for 24h. Results are expressed as mean ± SD. *p<0.05; **p<0.01; ***p<0.001.

At the higher concentration tested (50 μM) all of the compounds induced a significant increase in cell death (p<0.05). Nevertheless, only Auphen and Auterpy differed significantly from control at lower concentrations being thus, the most potent inducers of cell death (Figure 3.1).

The most potent compounds were also tested after 48h of incubation with similar, although potentiated, results (data not shown). Results were also in accordance to those observed by Hoechst staining (data not shown). Of note, it was not possible to identify viable cells after incubation with the highest concentration (50 μM), when analyzing Hoechst staining. From this small library of metallodrugs, and based on previous results, Auphen aroused as the most potent inducer of cellular death, followed by Auterpy. Despite the modest results obtained for both Aubipy and Audien, only the last one was excluded from the library under study. It was

replaced by an analogue of Auphen, which was also described as a potent and selective inhibitor of AQP3 – Cuphen. (Martins, 2013) As result of this modification in the library under study we were able to infer about the role of the metal ion on the effects of these metallodrugs in cellular viability.

3.1.2. MTS assay

We continued our metallodrugs cytotoxicity screening using the MTS viability assay. A431 cells were incubated with Auphen, Auterpy, Cuphen, AubipyMe and Aubipy in concentrations ranging from 0.250 µM up to 60 µM.

These results allowed a deeper analysis on the cytotoxic effects induced by these compounds. Dose-response curves were traced for both incubation periods (Figure 3.2), with results obtained from the data fits being summarized in Table 3.1.

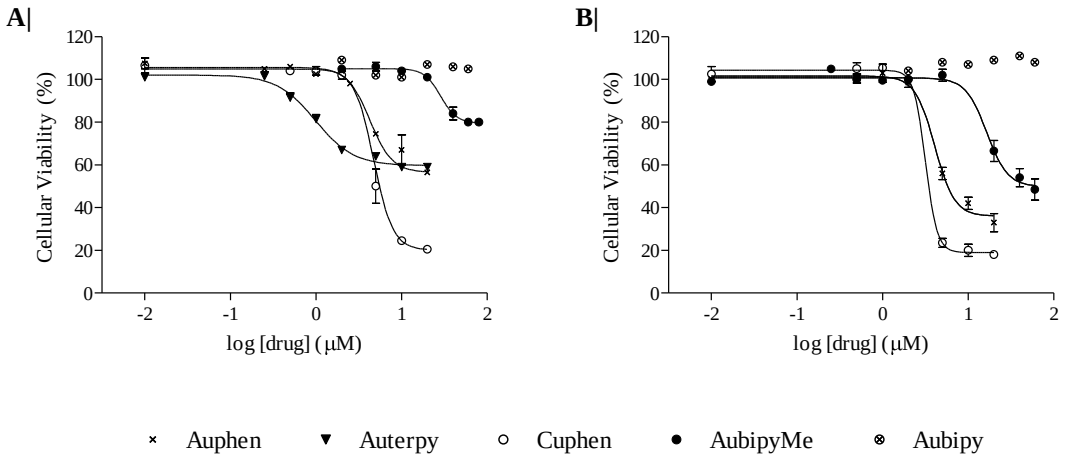

Figure 3.2. Concentration-dependent inhibition of A431 cellular viability by different metallodrugs after A| 48h and B| 72h of incubation. Results are expressed as mean percentage (%) of control ± SD.

After 48h of incubation (Figure 3.2A) only Cuphen exerted sufficient cytotoxicity in order to decrease 50% of cellular viability. On the other hand, Aubipy did not exert any effect on the viability of this cancer cell line. By increasing the incubation time, the cytotoxicity of these compounds was potentiated. Figure 3.2B shows the dose-response curves obtained for Auphen, Cuphen, Aubipy and AubipyMe after an incubation period of 72h. Comparing the evolution of the curves it is possible to proceed with a double comparison. First, it can be observed that at 50% of cellular viability, the concentration values for the phenantroline compounds (Auphen and Cuphen) are quite similar, suggesting a similar IC_{50} value. Both traces differ significantly for the one obtained for AubipyMe, where higher concentrations were needed to induce 50% of

cellular death. Second, Cuphen induces cellular death at a higher extension when compared to Auphen and AubipyMe, maintaining a cytotoxic profile very similar to the one obtained for the 48h incubation period. This copper compound induces a decrease in cellular viability of approximately 80%, while Auphen is only capable of a 65% reduction. No curves were obtained for this range of concentrations and time of incubation for Auterpy and Aubipy. Aubipy was not able to exert any effect on the cellular viability even at the highest concentration of 60 µM and regarding Auterpy, a different range of concentrations should be considered. Thus, it was not possible to determine the IC_{50} values for these compounds.

Table 3.1. Half-inhibitory concentrations for the cellular proliferation in A431 cells.

Compound	Timepoint (h)			
	48		72	
	IC_{50} ± SE (µM)	**R^2**	**IC_{50} ± SE (µM)**	**R^2**
Auphen	n.d.	(-)	3.7 ± 1.2	0.990
Auterpy	n.d.	(-)	n.d.	(-)
Cuphen	4.3 ± 1.1	0.988	3.0 ± 0.4	0.999
Aubipy	n.d.	(-)	n.d.	(-)
AubipyMe	n.d.	(-)	14.9 ± 1.1	0.995

Results obtained from three independent experiments. R^2 - Average linear correlation coefficients obtained by data curve fits.

Taken into account the results above, the cytotoxic potential of the studied metallodrugs, regarding this human epidermoid carcinoma cell line, can be represented in the following order: Cuphen > Auphen > AubipyMe.

Regarding Cuphen and Auphen, it is worth observing that the similarity of their cytotoxic effects is justifiable by their analogue structures, differing only in the metal core. In 1996, 1,10-phenanthroline was described as an inducer of DNA fragmentation in isolated rat-liver nuclei. Thus, cytotoxic effects can also be attributed to this complexing agent (Burkitt, 1996) in addition to the metal ion, which affords for the differences in cytotoxic activity between these two compounds.

Based on the above results, Cuphen was the molecule chosen to pursue in the present thesis. In addition to the high cytotoxic effect in A431 cells, it is important to refer that copper-phenantroline complexes are being described since 1979 as potent inducers of oxidative DNA damage. (Sigman, 1979, 1996; Bales, 2005) and Cu(II) ions are already described in literature as inhibitors of AQP3. (Zelenina, 2004) Moreover, this metallodrug is constituted by a metal ion which is physiologically accepted turning Cuphen as a very promising molecule to be further tested in a murine melanoma model. In order to stabilize this aquaporin inhibitor, allowing its *in*

vivo administration and targeting to tumors, this molecule was subsequently formulated in liposomes. These DDS are biodegradable, they are able to improve drug solubility, to protect the incorporated drug from premature degradation or metabolization while keeping its therapeutic activity. They also may change the PK and BD profiles of incorporated drug and consequently increasing the therapeutic efficacy. In addition, liposomes, depending on their lipid constituents, may reduce MPS capture and, taking the advantage of the impaired vasculature of tumors, may extravasate and accumulate in affected sites.

Table 3.2. Cuphen physical properties.

Chemical Structure	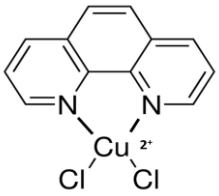
Melting point	No data available
MW	314.66
Partition coefficient: n-octanol/water	No data available

Dichloro(1,10-phenanthroline)copper(II); MSDS No. 362204: Sigma-Aldrich St. Louis, MO, USA, May 17, 2013, http://www.sigmaaldrich.com/catalog/product/aldrich/362204 (accessed October 20, 2013).

3.2. Optimization of methodologies for Cuphen quantification

As mentioned on chapter *2. Materials and Methods*, Cuphen was quantified by UV-spectrophotometry. To determine the wavelength of maximum absorption, serial dilutions were performed with EtOH and UV/Vis spectra were traced. In Figure 3.3 are shown the absorption spectra ranging from 200 to 800 nm and in a narrower range from 240 to 340 nm, respectively.

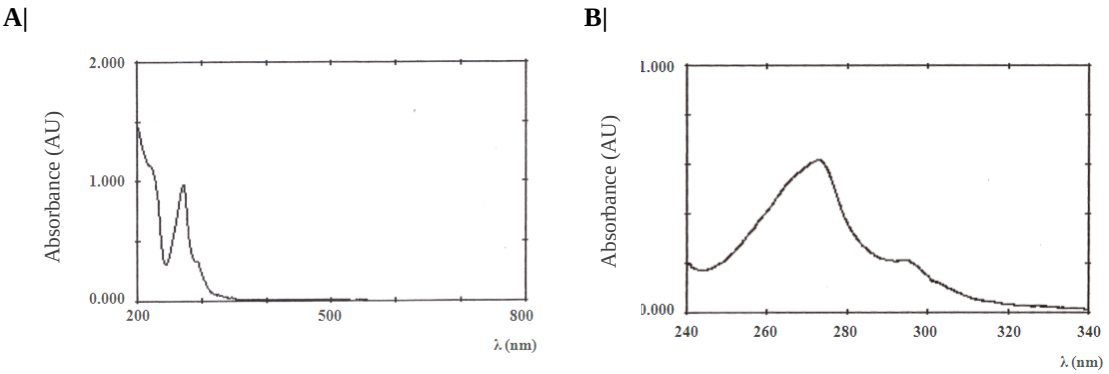

Figure 3.3. UV spectra obtained for Cuphen solution at two different concentrations and wavelength ranges. Spectrum traced with a Cuphen solution of **A|** 20uM; **B|** 10uM. Absorbance maximum recorded at 272nm.

After establishment of the appropriate wavelength for Cuphen, calibration curves were constructed using different concentrations ranging from 2 µM up to 20 µM. In Figure 3.4 a graphical representation of the calibration curves obtained for several independent experiments is shown.

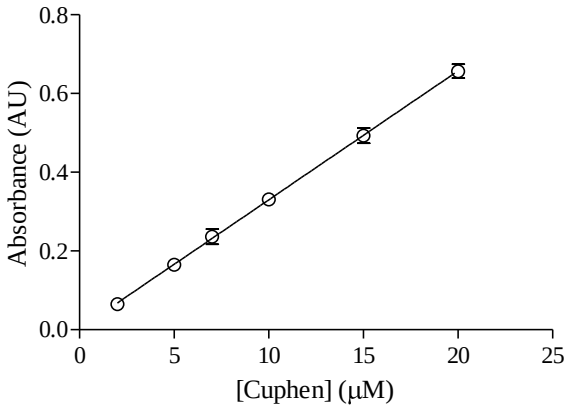

Figure 3.4. Graphical representation of data sets of calibration curves for Cuphen. Data are represented as mean ± S.D. of several independent experiments (n=12). R^2 - linear correlation coefficient: 0.9983; Slope: 0.0331 ± 0.0017; Y-intercept (x=0): 0.0001 ± 0.0020.

The obtained values evidence a high linearity and reproducibility in the selected range from different independent experiments.

3.3. Cuphen liposomes

Liposomes were prepared by the dehydration-rehydration method followed by an extrusion step to reduce the mean size of the so formed vesicles. (Cruz, 1993; Gaspar, 1996, 2008) Once Cuphen presents hydrophilic character it was only added after formation of the lipidic film. Its incorporation occurs after formation of the lipidic film which is hydrated by the Cuphen solution (deionized water). Following the lyophilization (overnight) the rehydration step was performed with HEPES buffer in two steps, in order to increase Cuphen incorporation. (Lasch, 2003) The extrusion of liposomal suspensions was performed in order to reduce and homogenize the mean size of the lipid suspension. Being a hydrophilic molecule the non incorporated material was removed by ultracentrifugation.

3.3.1. Characterization of Cuphen liposomes

Cuphen liposomes were prepared with different lipid compositions, i.e. phospholipids of different phase transition temperatures (Tc), with the aim to select the ones that were able to accommodate higher amounts of Cuphen per mol of lipid. Three neutral phospholipids - PC, DMPC and DPPC were used as major constituents of Cuphen nanoformulations that present increasing Tc of -6, +23, +41ºC, respectively.
The inclusion of positively charged surfactant, SA, was also considered and the influence of its presence in Cuphen incorporation parameters was compared with neutral nanoformulations. In addition, as it is our intention to develop long circulating liposomes, another set of lipid compositions containing the polymer PEG was also prepared.

The first series of nanoformulations was based on the natural phospholipid PC. In terms of charge this is a neutral phospholipid with a Tc of -6ºC. Considering its fluidity, Chol was included in the lipid composition to decrease the membrane permeability and consequently to enhance the stability of the incorporated Cuphen.
In Table 3.3 the results obtained for different PC Cuphen formulations are summarized.

Table 3.3. Physicochemical characterization of Cuphen liposomes: PC-based vesicles.

Formulation	Lipid Composition (molar ratio)	(Cuphen/Lip)i (nmol/µmol)	(Cuphen/Lip)f (nmol/µmol)	IE (%)	Ø (µm) (P.I.)	Zeta Pot. (mV)
1	PC	34 ± 5	21 ± 7	54 ± 1	0.15 (<0.15)	-9 ± 1
2	PC:Chol:PEG (1.85:1:0.15)	39 ± 4	15 ± 3	47 ± 5	0.16 (<0.15)	-4 ± 1
3	PC:Chol (2:1)	39 ± 3	17 ± 2	44 ± 2	0.20 (<0.10)	-9 ± 1
4	PC:SA (9.5:0.5)	36 ± 1	22 ± 5	61 ± 1	0.16 (<0.15)	-9 ± 1

Initial lipid concentration [Lip]i – 20 µmol/mL; Initial Cuphen [Cuphen]i – 500 nmol/mL;
PC transition temperature: -6ºC (Gunstone, 1986)
I.E. (%) – Incorporation efficiency, [(Cuphen/Lip)f] / [(Cuphen/Lip)i] x 100;
Ø – mean size of liposomes; P.I. – polydispersity index; Zeta Pot. – Zeta Potential.
Results are expressed as mean ± S.D.

All Cuphen liposomes presented mean sizes ranging from 0.15 to 0.20 µm with polydispersion index (P.I.) below 0.2 evidencing the high homogeneity of all nanoformulations.

In terms of loading capacity, PC formulations without Chol (**F1** and **F4**) were able to accommodate high amounts of Cuphen per µmol of lipid. Regarding to I.E. obtained values ranged from 54 to 61%. The inclusion of Chol in the lipid composition led to a decrease on incorporation parameters of **F2** and **F3**. When included in the lipid composition of liposomes, Chol is inserted within bilayers competing with the accommodation of hydrophobic molecules. This finding is in accordance with literature (Blume, 1993; Constantino, 1993) suggesting that Cuphen, even presenting hydrophilic character, may also interact with the lipid bilayers, probably through phenantroline, leading to the I.E. values observed.

Interestingly, all formulations in the absence of PEG presented similar zeta potential values (-9 ± 1 mV). Even for **F4**, the inclusion of SA was not able to reduce the negative charge of liposomes. In order to clarify these observations unloaded liposomes with the same lipid composition of **F1** and **F2** were prepared and the results obtained are shown in Table 3.4.

Table 3.4. Physicochemical properties of unloaded PC-based vesicles.

Lipid composition (molar ratio)	Ø (µm) (P.I.)	Zeta Pot. (mV)
PC	0.14 (0.1)	-4 ± 1
PC:Chol:PEG (1.85:1:0.15)	0.14 (0.1)	-3 ± 1

Ø – mean size of liposomes; P.I. – polydispersity index;
Zeta Pot. – Zeta Potential.
Results are expressed as mean ± S.D.

According to these results, while for PC:Chol:PEG no differences on the zeta potential values were achieved (-3 ± 1 mV), the PC unloaded liposomes displayed less negative values (-4 ± 1 mV) than those observed for **F1** (-9 ± 1 mV).

The different physicochemical properties observed for **F1** and unloaded PC liposomes point out that Cuphen influences the superficial charge of the vesicles.

In the second set of liposomal formulations tested the main phospholipid constituent was DMPC which presents a Tc of +23ºC. The influence of PEG and SA inclusion on Cuphen incorporation parameters was also evaluated and results are shown in Table 3.5.

Table 3.5. Physicochemical characterization of Cuphen liposomes: DMPC-based vesicles.

Formulation	Lipid Composition (molar ratio)	(Cuphen/Lip)i (nmol/µmol)	(Cuphen/Lip)f (nmol/µmol)	IE (%)	Ø (µm) (P.I.)	Zeta Pot. (mV)
5	DMPC	33 ± 10	3 ± 2	8 ± 3	0.19 (<0.15)	-1 ± 1
6	DMPC:Chol:PEG (1.85:1:0.15)	32 ± 12	3 ± 1	9 ± 1	0.19 (<0.20)	-3 ± 1
7	DMPC:SA (9.5:0.5)	42 ± 20	3 ± 2	6 ± 2	0.18 (<0.15)	+7 ± 1
8	DMPC:SA (9:1)	27 ± 5	2 ± 1	6 ± 2	0.16 (<0.20)	+18 ± 2

Initial lipid concentration [Lip]i – 20 µmol/mL; Initial Cuphen [Cuphen]i – 500 nmol/mL;
DMPC transition temperature: +23ºC (Gunstone, 1986)
I.E. (%) – Incorporation efficiency, [(Cuphen/Lip)f] / [(Cuphen/Lip)i] x 100;
Ø – mean size of liposomes; P.I. – polydispersity index; Zeta Pot. – Zeta Potential.
Results are expressed as mean ± S.D.

All Cuphen liposomal formulations presented mean sizes ranging from 0.16 to 0.19 μm with polydispersion index (P.I.) below 0.2.

Very low incorporation values, below 10%, were obtained for all tested formulations irrespective of charge or presence of PEG in the lipid composition.

The zeta potential values observed for these nanoformulations were in accordance to the expected values (i.e. with the charge of constituents) where the i) neutral phospholipid confers a charge of about zero; ii) PEG confers a negative charge of approximately -3mV and iii) liposomes become positively charged in the presence of increasing molar ratio of SA. While for **F4** negative values were observed when SA was included in the lipid composition, in this set of experiments **F7** and **F8** did not show the same feature.

As performed for PC-based vesicles, unloaded liposomes were also prepared and results are shown in Table 3.6.

Table 3.6. Physicochemical properties of unloaded DMPC-based vesicles.

Lipid composition (molar ratio)	**Ø (μm) (P.I.)**	**Zeta Pot. (mV)**
DMPC	0.16 (<0.15)	-2 ± 1
DMPC:Chol:PEG (1.85:1:0.15)	0.15 (<0.15)	-3 ± 1
DMPC:SA (9.5:0.5)	0.16 (<0.15)	+6 ± 1
DMPC:SA (9:1)	0.15 (<0.15)	+18 ± 2

Ø – mean size of liposomes; P.I. – polydispersity index;
Zeta Pot. – Zeta Potential.
Results are expressed as mean ± S.D.

According to these results, no differences on the zeta potential values were observed for loaded and unloaded liposomes, particularly for DMPC:SA formulations. This fact might be due to the low incorporation parameters obtained for these nanoformulations and consequently the ability of Cuphen to interfere with the superficial charge is diminished.

In the third set of liposomal formulations tested the main phospholipid constituent was DPPC which presents a Tc of +41ºC. The influence of PEG and SA inclusion on Cuphen incorporation parameters was evaluated and results are shown in Table 3.7.

Table 3.7. Physicochemical characterization of Cuphen liposomes: DPPC-based vesicles.

Formulation	Lipid Composition (molar ratio)	(Cuphen/Lip)i (nmol/µmol)	(Cuphen/Lip)f (nmol/µmol)	IE (%)	Ø (µm) (P.I.)	Zeta Pot. (mV)
9	DPPC	27 ± 5	2 ± 2	6 ± 3	0.8 (1.0)	-1 ± 1
10	DPPC:Chol:PEG (1.85:1:0.15)	35 ± 9	4 ± 2	10 ± 4	0.2 (<0.10)	-3 ± 1
11	DPPC:SA (9:1)	23 ± 4	2 ± 1	5 ± 3	0.8 (1.0)	+16 ± 1

Initial lipid concentration [Lip]i – 20 µmol/mL; Initial Cuphen [Cuphen]i – 500 nmol/mL;
DPPC transition temperature: +41 ºC (Gunstone, 1986)
I.E. (%) – Incorporation efficiency, [(Cuphen/Lip)f] / [(Cuphen/Lip)i] x 100;
Ø – mean size of liposomes; P.I. – polydispersity index; Zeta Pot. – Zeta Potential.
Results are expressed as mean ± SD.

These DPPC-based vesicles displayed high mean sizes and P.I. values. During extrusion step, higher pressures were necessary to apply even being performed at a temperature of +50ºC, when compared to those used for PC and DMPC formulations.

F9 and **F11** were totally polydispersed according to the P.I. values that reached its maximum. Very low incorporation parameters, below 10%, were also obtained for DPPC–based vesicles, and zeta potential values observed were in accordance with the charge of lipid constituents.

In conclusion and taking into account all the results presented in Tables 3.3-3.7, the incorporation of Cuphen in liposomes was dependent on the rigidity of the phospholipid and on the presence of Chol as shown in Figure 3.5. The presence of Chol and the higher the Tc of the phospholipid used led to a systematic decrease on Cuphen incorporation parameters.

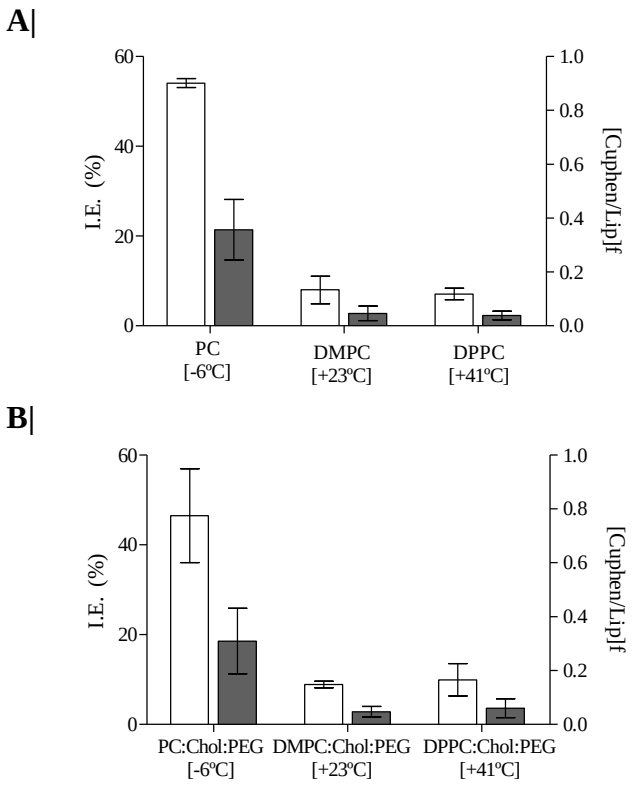

Figure 3.5. Influence of the bilayer rigidity on Cuphen incorporation parameters: I.E. (%) (white columns) and [Cuphen/Lip]f (grey columns). Comparison between **A|** PC, DMPC and DPPC (F1, F5 and F9); **B|** PC:Chol:PEG, DMPC:Chol:PEG and DPPC:Chol:PEG (F2, F6 and F10). Results are expressed as mean ± S.D.

For pursuing *in vitro* tests the selected formulations were those prepared with PC (**F1**) and PC:Chol:PEG (**F2**) as they presented higher I.E. Although similar incorporation parameters were achieved for PC:SA they were not chosen for *in vitro* studies due to SA toxicity as reported in literature. (Takano, 2003; Epstein-Barash, 2010)

3.4. *In vitro* cytotoxicity of Cuphen formulations

The cytotoxic effect of Cuphen in the free and liposomal forms was evaluated against two different cell lines: the A431, already used in the first set of experiments, and the murine colon cancer cells, C26. The rational for choosing the C26 cell line was based on the fact related with i) the expression of AQP3 in colonic surface epithelium (Ma, 1999) and ii) as well as on the evidence of AQP3 overexpression in human colorectal tumors. (Moon, 2003)

Here, the cytotoxic potential of this AQP3 inhibitor in the free and liposomal forms was assessed by MTS method for at least two different incubation periods (24, 48, 72 or 96h). These *in vitro* methodologies were already optimized and published. (Calado, 2012)
Negative control was constituted by the cell line under study in the presence of the culture medium. Unloaded liposomes also constituted another control group, using the same lipid concentrations as in loaded liposomes.

3.4.1. Cytotoxicity of Cuphen against A431 cells

For this human epidermoid carcinoma cell line, cells were incubated for 48 and 72h with Cuphen concentrations ranging from 0.625 μM up to 50 μM.

Cuphen in free form

After 48 and 72h of incubation with Cuphen in free form, significant cytotoxic effects were obtained as shown in Figure 3.6, by the dose-response curves traced.

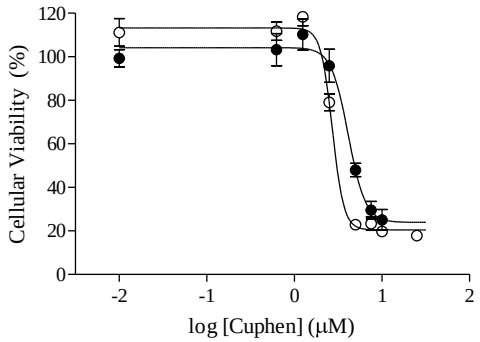

Figure 3.6. Concentration-dependent inhibition of A431 cells proliferation after different times of incubation with Cuphen in the free form. (●) – 48h; (○) – 72h. Results are expressed as mean percentage (%) of control ± SD.

Through the dose-response curves and at both incubation times, Cuphen was able to induce approximately 85% of cellular death, depending on the incubation period. In Table 3.8 the IC_{50} values determined based on the previous traces are shown: 4.1 ± 0.4 and 2.7 ± 0.1 μM 48 and 72h after incubation, respectively. The IC_{50} values are in accordance with the results obtained in the preliminary assay (p.34-35).

Table 3.8. Inhibition of the cellular proliferation of A431 cells by Cuphen in free form. Half-inhibitory concentrations.

Timepoint (h)	IC_{50} ± SE (μM)	R^2
48	4.1 ± 0.4	0.970
72	2.7 ± 0.1	0.991

Results obtained from several independent experiments. R^2 - Average linear correlation coefficients obtained by data curve fits.

In order to compare the cytotoxic effect induced by this AQP3 inhibitor, cellular viability 48 and 72h after incubation with 5 μM of Cuphen is discriminated in Figure 3.7.

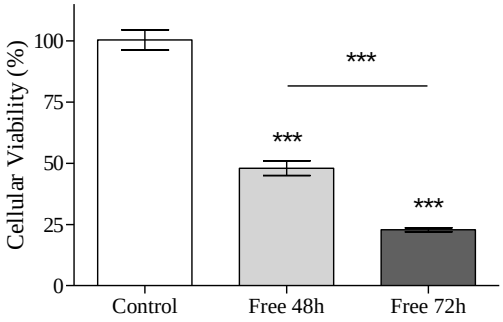

Figure 3.7. Graphical representation of A431 cells proliferation inhibition induced by Cuphen (5 μM) in free form 48 and 72h after incubation. Results are expressed as mean percentage (%) of control ± SD. ****p*<0.001.

The inhibition of cellular proliferation by Cuphen in the free form was statistically significant in comparison with control ($p<0.001$). After 48h of incubation with 5 μM of Cuphen, cellular viability was already below 50%. For a longer incubation period (72h) the metallodrug was able to induce cell death in an extension of about 80%.

Cuphen liposomes

The cytotoxic potential of Cuphen liposomes was also evaluated against this human epidermoid carcinoma cell line and compared to results obtained for the inhibitor in the free form. For this set of experiments, incubation times were 48 and 72h and drug concentrations ranged from i) 0.625 μM up to 50 μM for the free form and ii) 1.25 μM up to 50 μM for Cuphen liposomes. For unloaded liposomes, the lipid concentration range was the same as the one used in Cuphen liposomes.

Cuphen in the free form worked as a positive control, while unloaded liposomes and A431 cells constituted negative controls. The results obtained after 72h incubation period are shown in Figure 3.8.

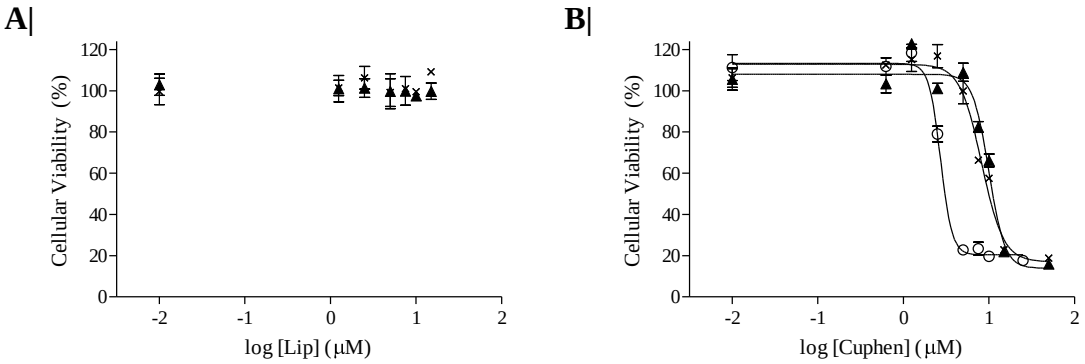

Figure 3.8. Concentration-dependent inhibition of 431 cells proliferation after 72h of incubation. A| Unloaded liposomes**; B|** Cuphen formulations. **(○) -** Free Cuphen; **(▲)** – PC Cuphen liposomes; (x) – PC:Chol:PEG Cuphen liposomes. Results are expressed as mean percentage (%) of control ± SD.

According to results displayed in Figure 3.8A, unloaded liposomes, using the same lipid concentration range as in Cuphen liposomes, did not exert any effect on the viability of A431 cells after the longest incubation period. In Figure 3.8B, Cuphen liposomes were able to induce cell death at low micromolar range. However the IC_{50} was slightly higher than the one observed for Cuphen in the free form. Moreover, both liposomal formulations **F1** and **F2** showed similar cytotoxic effect against this epidermoid carcinoma cell line, as seen by the virtually overlapped curves. This fact is also easily seen through Figure 3.9 and Table 3.9, where the IC_{50} values are shown. The slight increase on IC_{50} values for Cuphen in liposomal form suggests that metallodrug remains partially incorporated in liposomes. The same observation was also reported in literature for other antitumor drugs after incorporation in liposomes. (Fens, 2008)

Table 3.9. Inhibition of the cellular proliferation of A431 cells by Cuphen liposomes. Half-inhibitory concentrations.

Formulation	Timepoint (h)	IC_{50} ± SE (μM)	R^2
PC	48	11.4 ± 1.1	0.905
	72	10.0 ± 0.8	0.934
PC:Chol:PEG	48	10.7 ± 1.0	0.925
	72	8.3 ± 0.8	0.940

Results obtained from several independent experiments. R^2 - Average linear correlation coefficients obtained by data curve fits.

Summarizing, Cuphen nanoformulations incorporated in PC and PC:Chol:PEG, presented IC_{50} values of 10.0 ± 0.8 and 8.3 ± 0.8 μM, respectively after a 72h of incubation period. The linear correlation coefficients, R^2, were superior to 0.900 for all the experiments.

The cytotoxicity induced by Cuphen formulations, in free and liposomal forms was compared for a concentration of 15 μM following 48 and 72 h incubation period. Results are shown in Figure 3.9.

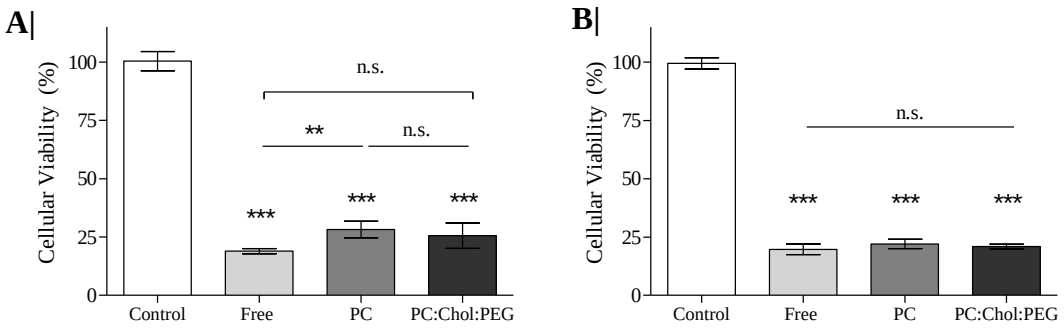

Figure 3.9. Graphical representation of A431 cells proliferation inhibition induced by Cuphen in free and liposomal forms at 15 μM. Different incubation times were tested **A|** 48 and **B|** 72h**.** Results are expressed as mean percentage (%) of control ± SD. **p*<0.05; ***p*<0.01**;** ****p*<0.001; n.s.: not statistically significant.

Following a 48h incubation period, Cuphen in free and liposomal forms displayed cytotoxic effect against A431 cells showing a significant viability decrease of approximately 70 and 75% for Cuphen liposomes (*p*<0.001) in comparison with control. For this incubation period and for a Cuphen concentration of 15 μM statistically significant differences (*p*<0.01*)* were only observed between free Cuphen and Cuphen incorporated in PC liposomes according to Figure 3.9A.

Following the 72h of incubation period and according to results in Figure 3.9B no significant differences were observed between all Cuphen formulations.

3.4.2. Cytotoxicity of Cuphen against C26 cells

Cuphen in free form

The cytotoxic effect of Cuphen against the colon cancer cell line, the C26, was evaluated following incubation periods of 24, 48, 72 and 96h.

The first approach in terms of *in vitro* studies was performed with this AQP3 inhibitor in free form in order to evaluate its potential cytotoxic activity against C26 cells. Incubation times of 24, 48, 72 and 96h were tested with concentrations ranging from 0.625 μM up to 50 μM.

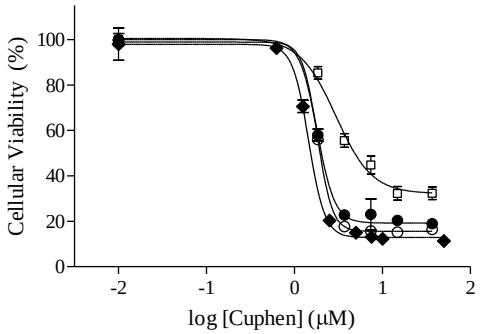

Figure 3.10. Concentration-dependent inhibition of C26 cells proliferation after different times of incubation with Cuphen in the free form. **(□) –** 24h; **(●)** – 48h; **(○)** – 72h; **(♦)** – 96h. Results are expressed as mean percentage (%) of control ± SD.

According to the results obtained (Figure 3.10) progress curves are very similar 48, 72 and 96h after Cuphen incubation. These results point to a high response C26 cells to this AQP3 inhibitor according to IC_{50} values obtained and shown in Table 3.10.

Table 3.10. Inhibition of the cellular proliferation of C26 cells by Cuphen in free form. Half-inhibitory concentrations.

Timepoint (h)	IC_{50} ± SE (μM)	R^2
24	3.0 ± 0.4	0.981
48	2.1 ± 0.2	0.986
72	1.8 ± 0.1	0.998
96	1.5 ± 0.1	0.997

Results obtained from several independent experiments. R^2 - Average linear correlation coefficients obtained by data curve fits.

Cuphen proved to be quite effective by inhibiting the proliferation of this cancer cell line leading to IC_{50} values in low micromolar range.

Upon verification of the cytotoxic activity of Cuphen, in the free form, against this cancer cell line, liposomal formulations were also tested.

Taking into account that Cuphen incorporated in liposomes is not immediately available for exerting its cytotoxic effect, the 24h of incubation period was not considered in the following experiments.

Cuphen Liposomes

Pursuing the idea of evaluating Cuphen liposomes efficiency against C26 murine cancer cell line, several independent experiments (six samples for each concentration under study) were performed. For this set of experiments, drug concentrations ranged from i) 0.625 μM up to 50 μM for the free form and ii) 1.25 μM up to 50 μM for Cuphen liposomes. For unloaded liposomes, the lipid concentration range was the same as the one used in Cuphen liposomes.

In order to estimate a possible improvement in the cytotoxic effect imposed by Cuphen liposomes the 96h incubation period was considered in addition to 48 and 72h timepoints. Cuphen in the free form worked as a positive control, while unloaded liposomes and C26 cells constituted negative controls. Figure 3.11 shows the representative dose-response curves traced for this set of experiments.

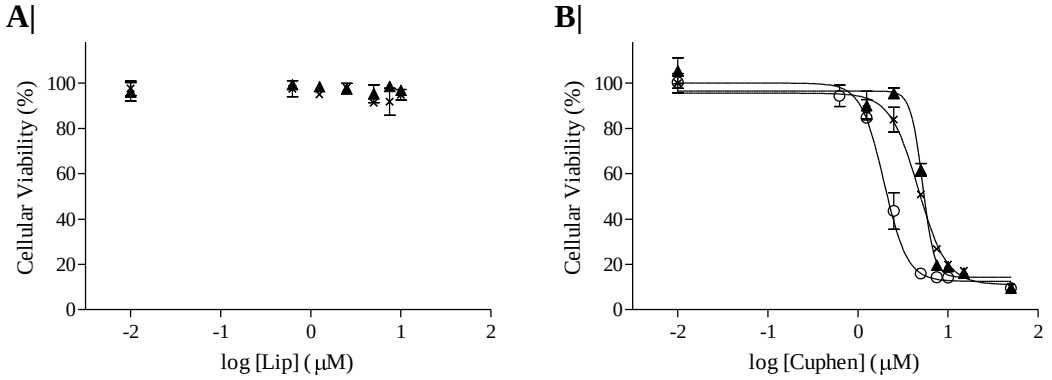

Figure 3.11. Concentration-dependent inhibition of C26 cells proliferation after 72h of incubation. A| Unloaded liposomes; **B|** Cuphen formulations. **(○) -** Free Cuphen; **(▲)** – PC Cuphen liposomes; (x) – PC:Chol:PEG Cuphen liposomes. Results are expressed as mean percentage (%) of control ± SD.

According to results displayed in Figure 3.11A, unloaded liposomes, using the same lipid concentration range as in Cuphen liposomes, did not exert any effect on the viability of C26 cells after the 72h incubation period.

In Figure 3.11B, Cuphen liposomes were able to induce cell death at low micromolar concentrations range. Cytotoxic profiles are similar to those obtained for A431 cells (*see* Figure 3.8). The half-inhibitory concentrations are show below, in Table 3.11.

Table 3.11. Inhibition of the cellular proliferation of C26 cells by Cuphen liposomes. Half-inhibitory concentrations.

Formulation	Timepoint (h)	IC_{50} ± SE (μM)	R^2
PC	48	7.3 ± 0.7	0.953
	72	5.8 ± 0.4	0.966
	96	5.4 ± 0.2	0.995
PC:Chol:PEG	48	7.3 ± 1.0	0.970
	72	4.4 ± 0.4	0.989
	96	4.2 ± 0.1	0.998

Results obtained from several independent experiments. R^2 - Average linear correlation coefficients obtained by data curve fits.

From the results expressed in Table 3.11, IC_{50} values for both liposomal formulations at 48, 72 and 96h incubation periods ranged from 4 to 7 μM.

For this set of experiments and 72h after incubation, Cuphen formulations, prepared with PC and PC:Chol:PEG, presented IC_{50} values of 5.8 ± 0.4 and 4.4 ± 0.4 μM, respectively. For the free form and after the same incubation time the IC_{50} was of 1.9 ± 0.1 μM, which is in accordance to the result previously obtained. For all experiments, the linear correlation coefficients, R^2, were higher than 0.950.

The cytotoxicity induced by Cuphen formulations, in free and liposomal forms was compared for a concentration of 10 μM following 48, 72 and 96h incubation period. Results are shown in Figure 3.12.

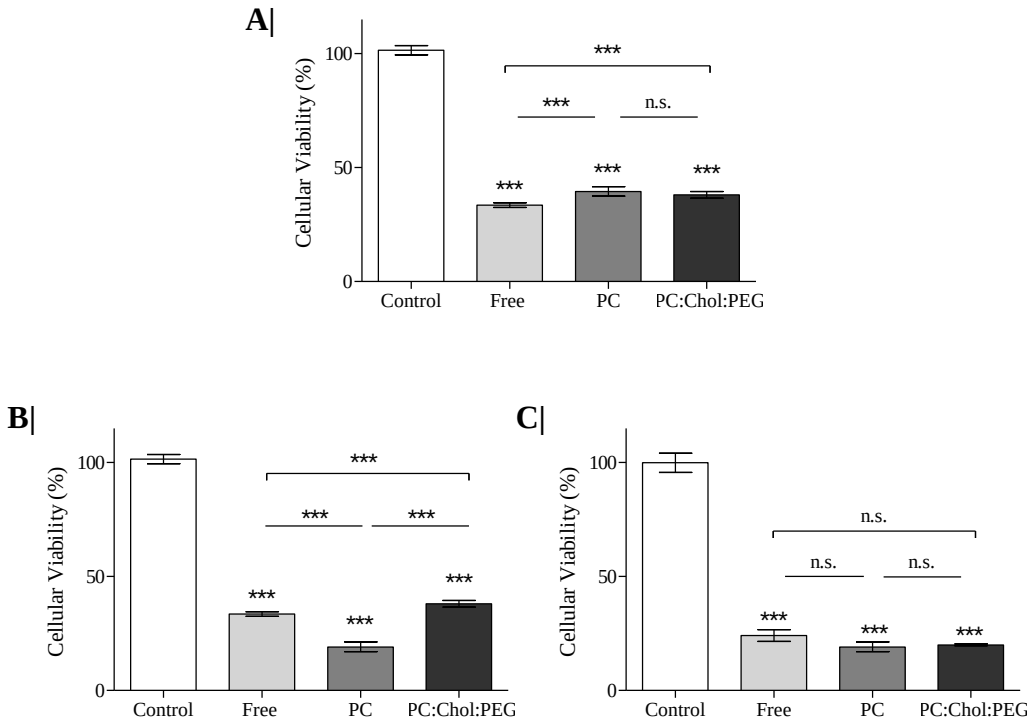

Figure 3.12. Graphical representation of C26 cells proliferation inhibition induced by Cuphen in free and liposomal forms at 10 µM. Different incubation times were tested: **A|** 48h; **B|** 72h and **C|** 96h. Results are expressed as mean percentage (%) of control ± SD. ***p<0.001; n.s.: not statistically significant.

As shown in Figure 3.12, after the 48h incubation period Cuphen liposomes were able to induce more than 50% of cellular death. Interestingly, Cuphen incorporated in PC and PC:Chol:PEG did not show statistically significant differences (p>0.05*)* in terms of cytotoxic effect (Figure 3.12A). For the remaining incubation times studied it was expected to achieve similar results, with a progressive increase on cell death. However, for the 72h incubation period, PC Cuphen liposomes showed a significant improvement (p<0.001) in terms of cytotoxic activity when compared to PEG liposomes or even Cuphen in free form as seen in Figure 3.12B. This fact may be justified by the liposome constitution. Phosphatidylcholine, a more fluid lipid, yields a more fluid membrane that may enable Cuphen release in a shorter period of time. On the other hand, the results obtained for PEG liposomal formulation suggest that Cuphen still remains partially incorporated in the lipid system.

Nevertheless, for the 96h incubation period (Figure 3.12C) Cuphen incorporated in PC and PEG liposomes displayed similar cytotoxic effect (p>0.05) inducing cell death at an extension of about 80%, as observed for the free molecule.

3.5. Storage stability of Cuphen liposomes

In general, liposomal formulations are not produced to be stored in suspension for more than two weeks. The incorporated material may be released or chemical or physical instability of the phospholipids may occur. In addition, aqueous formulations tend to suffer hydrolytic degradation. (Kensil, 1981) The best storage condition for liposomes is the lyophilized form. (Frrkjaer, 1982) Using adequate lyophilization conditions it is possible to ensure the preservation of physicochemical properties of liposomal formulations.

With the aim to evaluate the stability of Cuphen, in suspension, after incorporation in liposomes, its content was determined after a storage period of 10 days and compared with time zero, according to the following formula: $[(\text{Cuphen/Lip})_{t=10}/(\text{Cuphen/Lip})_{t=0}] \times 100$.

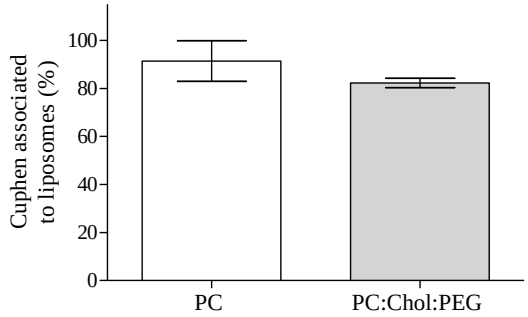

Figure 3.13. Cuphen liposomes stability after storage at 4ºC for 10 days. Data from two independent experiments. Results are expressed as mean ± SD.

As shown in Figure 3.13, PC and PC:Chol:PEG formulations are very stable as, particularly for PC, more than 90% of the incorporated Cuphen was still associated to liposomes 10 days after their preparation.

Table 3.12. Physicochemical properties of Cuphen liposomes after 10 days in suspension.

Formulation	t=0		t=10	
	Ø (µm) (P.I.)	**Zeta Pot. (mV)**	**Ø (µm) (P.I.)**	**Zeta Pot. (mV)**
PC	0.17 (<0.20)	-9 ± 1	0.18 (<0.20)	-9 ± 1
PC:Chol:PEG	0.16 (<0.20)	-4 ± 1	0.18 (<0.20)	-5 ± 1

Ø – mean size of liposomes; P.I. – polydispersity index;
Zeta Pot. – Zeta Potential.
Results are expressed as mean ± S.D.

In terms of mean size and zeta potential both formulations preserved their physicochemical properties as shown above in Table 3.12. These results reinforce the stability of the Cuphen liposomes in suspension after storage for 10 days.

4. Conclusions and Future Work

Since 1992, when the first water channel was reported, AQPs have been subject of intensive studies. Although this family of proteins still lacks a full and comprehensive characterization, several important physiological functions have already been reported. In fact, the last decade was marked by the discovery of different pathologies somehow associated to AQPs. Recently AQP3, which is highly expressed in skin keratinocytes, was implicated in physiological processes like skin hydration and wound healing. This protein permeates both water and glycerol and, when overexpressed, greatly increases the intracellular concentration of glycerol. As consequence, cells possess high pools of an energetic substrate that is also essential for lipid synthesis. Thus, all the requirements for cellular proliferation are gathered. In addition, water transport by this channel also affords for cellular migration, another important event in tumorigenesis. Altogether, AQP3 appears to act as a key player during skin tumorigenesis and should be considered a new player in skin cancer biology. Consequently, the search for selective inhibitors of AQP3 is now even more relevant. Based on the well known inhibition of AQPs by $HgCl_2$, and on the widely use of platinum in cancer therapy since the 80's, many other compounds have emerged ever since. However, their toxicity is extremely elevated and, particularly for mercury-based compounds, their possible benefits do not compensate the risk. Recently, our group reported different metallodrugs as potent and selective inhibitors of human AQP3 that can be further explored on *in vivo* studies. Interestingly, all of the compounds are described as cytotoxic agents.

The present work allowed us to conclude that Cuphen is a potent inhibitor of A431 and C26 tumor cells proliferation, presenting IC_{50} values of 3.0 ± 0.4 μM and 1.8 ± 0.1 μM after 72h of drug incubation, respectively. As the best lead compound from the small library of AQP3 inhibitors tested, this Cu(II) complex was selected to be incorporated in liposomes for future *in vivo* studies. After an optimization of the liposome preparation procedures, a systematic study using different lipid compositions was performed, aiming at the maximization of Cuphen incorporation parameters. Lipid mixtures containing PC and/or PEG allowed the achievement of incorporation efficiencies of approximately 50%. The association of Cuphen into liposomes was favored by fluid phospholipids, i.e. PC-based vesicles. Following the selection of the best formulations, Cuphen liposomes were tested *in vitro* against A431 and C26 cells. From these set of experiments we could conclude that the incorporation of Cuphen in liposomes was able to preserve the cytotoxic effect of this AQP3 inhibitor with IC_{50} values below 10 μM for both cancer cell lines, after 72h of incubation. Moreover, unloaded liposomes did not exert any effect on the viability of cancer cells, as intended for a drug carrier.

In view of these promising *in vitro* results, the establishment of a murine melanoma model to evaluate the therapeutic effect of Cuphen formulations should be considered.

Future work

The full understanding of the AQP3 role in skin tumorigenesis is still a distant reality. Notwithstanding, several efforts have been made in order to take advantage of the actual knowledge.

The results presented and discussed in this thesis allowed us to look and move forward with a new perspective for cancer therapy having AQP3 as putative drug target. Based on this work, experiments aiming at different approaches can now be designed.

The first approach will consist in the extension of the actual work to *in vivo* studies, through the establishment of an appropriate murine model allowing the evaluation of the therapeutic effect of Cuphen formulations. Additionally, the cellular membrane of a human melanoma cell line could be analyzed in order to explore possible useful characteristics for the optimization of drug targeting, in addition to the passive targeting that PEG implicates.

Another approach would be the utilization of these metallodrugs as AQP3 inhibitors in a broad sense, testing for example, the same liposomal formulations with lower drug loading, aiming at targeting the channel inhibition without cell death. This perspective could not only elucidate about the AQP3 inhibition itself but also enlarge the actual state of the art on AQP3-dependent tumorigenesis. For this particular case, *in silico* and *in vitro* studies could be performed in order to infer about AQP3 inhibition by the intracellular entrance of the pore. Permeability assays with Cuphen liposomes could be considered as well.

5. References

Agre P, Sasaki S, Chrispeels M. Aquaporins: a family of water channel proteins. *Am J Physiol* (1993); 265(3 Pt 2): F461.

Allen TM, Cullis PR. Drug delivery systems: entering the mainstream. *Science* (2004); 303(5665): 1818-1822.

Bales BC, Kodama T, Weledji YN, Pitie M, Meunier B, Greenberg MM. Mechanistic studies on DNA damage by minor groove binding copper-phenanthroline conjugates. *Nucleic Acids Res* (2005); 33(16): 5371-5379.

Bangham AD, Standish MM, Watkins JC. Diffusion of univalent ions across the lamellae of swollen phospholipids. *J Mol Biol* (1965); 13(1): 238-252.

Bei D, Meng J, Youan BB. Engineering nanomedicines for improved melanoma therapy: progress and promises. *Nanomedicine (Lond)* (2010); 5(9): 1385-1399.

Benedek TG. The history of gold therapy for tuberculosis. *J Hist Med Allied Sci* (2004); 59(1): 50-89.

Berners-Price SJ, Filipovska A. Gold compounds as therapeutic agents for human diseases. *Metallomics* (2011); 3(9): 863-873.

Bertolotti M, Bestetti S, Garcia-Manteiga JM, Medrano-Fernandez I, Dal Mas A, Malosio ML, Sitia R. Tyrosine kinase signal modulation: a matter of H2O2 membrane permeability? *Antioxid Redox Signal* (2013).

Bin K, Shi-Peng Z. Acetazolamide inhibits aquaporin-1 expression and colon cancer xenograft tumor growth. *Hepatogastroenterology* (2011); 58(110-111): 1502-1506.

Blume G, Cevc G. Molecular mechanism of the lipid vesicle longevity in vivo. *Biochim Biophys Acta* (1993); 1146(2): 157-168.

Burkitt MJ, Milne L, Nicotera P, Orrenius S. 1,10-Phenanthroline stimulates internucleosomal DNA fragmentation in isolated rat-liver nuclei by promoting the redox activity of endogenous copper ions. *Biochem J* (1996); 313 (Pt 1): 163-169.

Calado S. Nanoformulations of triazene analogues with specific affinity to human melanoma [Master's thesis]. Almada, Escola Superior de Saúde Egas Moniz 2012.

Carbrey J, Agre P. Discovery of the Aquaporins and Development of the Field. In: Handbook of Experimental Pharmacology Beitz E (Eds.). 190, Springer-Verlag, Berlin Heidelberg; 2009; pp. 3-28.

Casini A, Kelter G, Gabbiani C, Cinellu MA, Minghetti G, Fregona D, Fiebig HH, Messori L. Chemistry, antiproliferative properties, tumor selectivity, and molecular mechanisms of novel gold(III) compounds for cancer treatment: a systematic study. *J Biol Inorg Chem* (2009); 14(7): 1139-1149.

Castle N. Aquaporins as targets for drug discovery. *Drug Discovery Today* (2005); 10(7).

Constantino L, Cruz MEM, Mehta R, Lopez-Berestein G. Formulation and toxicity of liposomes containing Rifampicin. *Journal of Liposome Research* (1993); 3(2): 275-301.

Cory AH, Owen TC, Barltrop JA, Cory JG. Use of an aqueous soluble tetrazolium/formazan assay for cell growth assays in culture. *Cancer Commun* (1991); 3(7): 207-212.

Cruz MEM, Gaspar MM, Lopes F, Jorge JS, Perez-Soler R. Liposomal L-Asparaginase: in vitro evaluation. *Int. J. Pharm.* (1993); 96(1-3): 67-77.

Cruz MEM, Simões SI, Lopes F, Jorge JC, Perez-Soler R. Formulation of NPDDS for macromolecules. In: Drug delivery nanoparticles formulation and characterization. Yashwant Pathak DT (Eds.). 191(3), Informa Healthcare, New York; 2009; pp. 35-49.

Desoize B. Metals and metal compounds in cancer treatment. *Anticancer Res* (2004); 24(3a): 1529-1544.

Endo M, Jain RK, Witwer B, Brown D. Water channel (aquaporin 1) expression and distribution in mammary carcinomas and glioblastomas. *Microvasc Res* (1999); 58(2): 89-98.

Epstein-Barash H, Gutman D, Markovsky E, Mishan-Eisenberg G, Koroukhov N, Szebeni J, Golomb G. Physicochemical parameters affecting liposomal bisphosphonates bioactivity for restenosis therapy: internalization, cell inhibition, activation of cytokines and complement, and mechanism of cell death. *J Control Release* (2010); 146(2): 182-195.

Fens MH, Hill KJ, Issa J, Ashton SE, Westwood FR, Blakey DC, Storm G, Ryan AJ, Schiffelers RM. Liposomal encapsulation enhances the antitumour efficacy of the vascular disrupting agent ZD6126 in murine B16.F10 melanoma. *Br J Cancer* (2008); 99(8): 1256-1264.

Frrkjaer S, Hjorth EL, and Wrrts O. Stability and storage of liposomes. In: Optimization of Drug Delivery. Bundgaard H, Bagger Hansen A, and Kofod H., (Eds.), Munksgaard, Copenhagen; 1982; pp. 384.

Gao L, Gao Y, Li X, Howell P, Kumar R, Su X, Vlassov AV, Piazza GA, Riker AI, Sun D, Xi Y. Aquaporins mediate the chemoresistance of human melanoma cells to arsenite. *Mol Oncol* (2012); 6(1): 81-87.

Gaspar MM, Perez-Soler R, Cruz MEM. Biological characterization of L-asparaginase liposomal formulations. *Cancer Chemother Pharmacol* (1996); 38(4): 373-377.

Gaspar MM, Cruz A, Fraga AG, Castro AG, Cruz MEM, Pedrosa J. Developments on drug delivery systems for the treatment of mycobacterial infections. *Curr Top Med Chem* (2008); 8(7): 579-591.

Gregoriadis G, Ryman BE. Fate of protein-containing liposomes injected into rats. An approach to the treatment of storage diseases. *Eur J Biochem* (1972); 24(3): 485-491.

Guidi F, Landini I, Puglia M, Magherini F, Gabbiani C, Cinellu MA, Nobili S, Fiaschi T, Bini L, Mini E, Messori L, Modesti A. Proteomic analysis of ovarian cancer cell responses to cytotoxic gold compounds. *Metallomics* (2012); 4(3): 307-314.

Gunstone FD, Harwood JL, Padley FB. The Lipid Handbook, Chapman and Hall (Eds.). (1986)

Hara-Chikuma M, Verkman AS. Aquaporin-3 facilitates epidermal cell migration and proliferation during wound healing. *J Mol Med (Berl)* (2008a); 86(2): 221-231.

Hara-Chikuma M, Verkman AS. Prevention of skin tumorigenesis and impairment of epidermal cell proliferation by targeted aquaporin-3 gene disruption. *Mol Cell Biol* (2008b); 28(1): 326-332.

Hara-Chikuma M, Verkman AS. Roles of aquaporin-3 in the epidermis. *J Invest Dermatol* (2008c); 128(9): 2145-2151.

Hara M, Ma T, Verkman AS. Selectively reduced glycerol in skin of aquaporin-3-deficient mice may account for impaired skin hydration, elasticity, and barrier recovery. *J Biol Chem* (2002); 277(48): 46616-46621.

Harris JM, Chess RB. Effect of pegylation on pharmaceuticals. *Nat Rev Drug Discov* (2003); 2(3): 214-221.

Hu J, Verkman AS. Increased migration and metastatic potential of tumor cells expressing aquaporin water channels. *FASEB J* (2006); 20(11): 1892-1894.

Huber VJ, Tsujita M, Nakada T. Aquaporins in drug discovery and pharmacotherapy. *Mol Aspects Med* (2012).

Ishibashi K, Hara S, Kondo S. Aquaporin water channels in mammals. *Clin Exp Nephrol* (2009); 13(2): 107-117.

Kensil CR, Dennis EA. Alkaline hydrolysis of phospholipids in model membranes and the dependence on their state of aggregation. *Biochemistry* (1981); 20(21): 6079-6085.

King LS, Kozono D, Agre P. From structure to disease: the evolving tale of aquaporin biology. *Nat Rev Mol Cell Biol* (2004); 5(9): 687-698.

Kruse E, Uehlein N, Kaldenhoff R. The Aquaporins. *Genome Biology* (2006); 7(206).

Lasch J, Weissig V, Brandl M. Preparation of liposomes. In: Liposomes a pratical approach. Torchilin V.P. and Weissig V. (Eds.), Oxford Univ. Press Inc, New York; 2003; pp. 3-29.

Liu K, Nagase H, Huang CG, Calamita G, Agre P. Purification and functional characterization of aquaporin-8. *Biol Cell* (2006); 98(3): 153-161.

Lopez-Campos JL, Sanchez Silva R, Gomez Izquierdo L, Marquez E, Ortega Ruiz F, Cejudo P, Barrot Cortes E, Toledo Aral JJ, Echevarria M. Overexpression of Aquaporin-1 in lung adenocarcinomas and pleural mesotheliomas. *Histol Histopathol* (2011); 26(4): 451-459.

Ma T, Verkman AS. Aquaporin water channels in gastrointestinal physiology. *J Physiol* (1999); 517 (Pt 2): 317-326.

Machida Y, Ueda Y, Shimasaki M, Sato K, Sagawa M, Katsuda S, Sakuma T. Relationship of aquaporin 1, 3, and 5 expression in lung cancer cells to cellular differentiation, invasive growth, and metastasis potential. *Hum Pathol* (2011); 42(5): 669-678.

Maeda H, Wu J, Sawa T, Matsumura Y, Hori K. Tumor vascular permeability and the EPR effect in macromolecular therapeutics: a review. *J Control Release* (2000); 65(1-2): 271-284.

Maeda H, Sawa T, Konno T. Mechanism of tumor-targeted delivery of macromolecular drugs, including the EPR effect in solid tumor and clinical overview of the prototype polymeric drug SMANCS. *J Control Release* (2001); 74(1-3): 47-61.

Magni F, Sarto C, Ticozzi D, Soldi M, Bosso N, Mocarelli P, Kienle MG. Proteomic knowledge of human aquaporins. *Proteomics* (2006); 6(20): 5637-5649.

Martins AP, Marrone A, Ciancetta A, Galan Cobo A, Echevarria M, Moura TF, Re N, Casini A, Soveral G. Targeting aquaporin function: potent inhibition of aquaglyceroporin-3 by a gold-based compound. *PLoS One* (2012); 7(5): e37435.

Martins AP, Ciancetta A, de Almeida A, Marrone A, Re N, Soveral G, Casini A. Aquaporin Inhibition by Gold(III) Compounds: New Insights. *ChemMedChem* (2013); 8(7): 1086-1092.

Messori L, Abbate F, Marcon G, Orioli P, Fontani M, Mini E, Mazzei T, Carotti S, O'Connell T, Zanello P. Gold(III) complexes as potential antitumor agents: solution chemistry and cytotoxic properties of some selected gold(III) compounds. *J Med Chem* (2000); 43(19): 3541-3548.

Messori L, Marcon G. Gold complexes as antitumor agents. *Met Ions Biol Syst* (2004); 42: 385-424.

Miller EW, Dickinson BC, Chang CJ. Aquaporin-3 mediates hydrogen peroxide uptake to regulate downstream intracellular signaling. *Prot. Natl. Acad. Sci. U.S.A.* (2010); 107(36): 15681-15686.

Mirabelli CK, Johnson RK, Sung CM, Faucette L, Muirhead K, Crooke ST. Evaluation of the in vivo antitumor activity and in vitro cytotoxic properties of auranofin, a coordinated gold compound, in murine tumor models. *Cancer Res* (1985); 45(1): 32-39.

Moon C, Soria JC, Jang SJ, Lee J, Obaidul Hoque M, Sibony M, Trink B, Chang YS, Sidransky D, Mao L. Involvement of aquaporins in colorectal carcinogenesis. *Oncogene* (2003); 22(43): 6699-6703.

Nobili S, Mini E, Landini I, Gabbiani C, Casini A, Messori L. Gold compounds as anticancer agents: chemistry, cellular pharmacology, and preclinical studies. *Med Res Rev* (2010); 30(3): 550-580.

Preston GM, Carroll TP, Guggino WB, Agre P. Appearance of water channels in Xenopus oocytes expressing red cell CHIP28 protein. *Science* (1992); 256(5055): 385-387.

Riss TL, Moravec RA. Comparison of MTT, XTT, and a novel tetrazolium compound MTS for in vitro proliferation and chemosensitivity assays. *Mol. Biol. Cell (Suppl.)* (1992); 3: 184a.

Rojek A, Praetorius J, Frokiaer J, Nielsen S, Fenton RA. A current view of the mammalian aquaglyceroporins. *Annu Rev Physiol* (2008); 70: 301-327.

Rosenberg B, Vancamp L, Krigas T. Inhibition of Cell Division in Escherichia Coli by Electrolysis Products from a Platinum Electrode. *Nature* (1965); 205: 698-699.

Rosenberg B, Vancamp L, Trosko JE, Mansour VH. Platinum compounds: a new class of potent antitumour agents. *Nature* (1969); 222(5191): 385-386.

Rouser G, Fkeischer S, Yamamoto A. Two dimensional then layer chromatographic separation of polar lipids and determination of phospholipids by phosphorus analysis of spots. *Lipids* (1970); 5(5): 494-496.

Saetern AM. Parenteral Liposome and Cyclodextrin Formulations of Camptothecin. [PhD's thesis]. Tromsø, Norway, University of Tromsø; 2004.

Serratrice M, Edafe F, Mendes F, Scopelliti R, Zakeeruddin SM, Gratzel M, Santos I, Cinellu MA, Casini A. Cytotoxic gold compounds: synthesis, biological characterization and investigation of their inhibition properties of the zinc finger protein PARP-1. *Dalton Trans* (2012); 41(11): 3287-3293.

Sigman DS, Graham DR, D'Aurora V, Stern AM. Oxygen-dependent cleavage of DNA by the 1,10-phenanthroline . cuprous complex. Inhibition of Escherichia coli DNA polymerase I. *J Biol Chem* (1979); 254(24): 12269-12272.

Sigman DS, Landgraf R, Perrin DM, Pearson L. Nucleic acid chemistry of the cuprous complexes of 1,10-phenanthroline and derivatives. *Met Ions Biol Syst* (1996); 33: 485-513.

Slingerland M, Guchelaar HJ, Gelderblom H. Liposomal drug formulations in cancer therapy: 15 years along the road. *Drug Discov Today* (2012); 17(3-4): 160-166.

Soveral G, Trincão J, Moura TF. Aquaporins: Membrane channels for water transport. *Canal BQ* (2011); 8: 36-43.

Takano S, Aramaki Y, Tsuchiya S. Physicochemical properties of liposomes affecting apoptosis induced by cationic liposomes in macrophages. *Pharm Res* (2003); 20(7): 962-968.

Takata K, Matsuzaki T, Tajika Y. Aquaporins: water channel proteins of the cell membrane. *Prog Histochem Cytochem.* (2004); 39(1): 1-83.

Torchilin VP. Recent advances with liposomes as pharmaceutical carriers. *Nat Rev Drug Discov* (2005); 4(2): 145-160.

Torchilin VP. Targeted pharmaceutical nanocarriers for cancer therapy and imaging. *AAPS J* (2007); 9(2): E128-147.

Vacca A, Frigeri A, Ribatti D, Nicchia GP, Nico B, Ria R, Svelto M, Dammacco F. Microvessel overexpression of aquaporin 1 parallels bone marrow angiogenesis in patients with active multiple myeloma. *Br J Haematol* (2001); 113(2): 415-421.

Verkman AS. More than just water channels: unexpected cellular roles of aquaporins. *J Cell Sci* (2005); 118(Pt 15): 3225-3232.

Verkman AS, Hara-Chikuma M, Papadopoulos MC. Aquaporins--new players in cancer biology. *J Mol Med (Berl)* (2008); 86(5): 523-529.

Verkman AS. Knock-out models reveal new aquaporin functions. In: Handb Exp Pharmacol. Beitz E (Eds.). 190, Springer-Verlag Berlin Heidelberg; 2009; pp. 359-381.

Verkman AS. Aquaporins at a glance. *J Cell Sci* (2011a); 124(Pt 13): 2107-2112.

Verkman AS, Ratelade J, Rossi A, Zhang H, Tradtrantip L. Aquaporin-4: orthogonal array assembly, CNS functions, and role in neuromyelitis optica. *Acta Pharmacol Sin* (2011b); 32(6): 702-710.

Verkman AS. Aquaporins in clinical medicine. *Annu Rev Med* (2012); 63: 303-316.

Verkman AS. Aquaporins. *Curr Biol* (2013); 23(2): R52-55.

Wspalz T, Fujiyoshi Y, Engel A. The AQP structure and functional implications. *Handb Exp Pharmacol* (2009); (190): 31-56.

Wu B, Beitz E. Aquaporins with selectivity for unconventional permeants. *Cell. Mol. Life Sci* (2007); 64(18): 2413 – 2421.

Zeidel ML, Ambudkar SV, Smith BL, Agre P. Reconstitution of functional water channels in liposomes containing purified red cell CHIP28 protein. *Biochemistry* (1992); 31(33): 7436-7440.

Zelenina M, Tritto S, Bondar AA, Zelenin S, Aperia A. Copper inhibits the water and glycerol permeability of aquaporin-3. *J Biol Chem* (2004); 279(50): 51939-51943.

Zeuthen T. How water molecules pass through aquaporins. *TRENDS in Biochemical Sciences* (2001); 26(2).